N 70 27166

NASA CR 109852

TRANSONIC FLOW IN A CONVERGING-DIVERGING NOZZLE

FINAL REPORT

Lockheed

MISSILES & SPACE COMPANY

A GROUP DIVISION OF LOCKHEED AIRCRAFT CORPORATION

SUNNYVALE, CALIFORNIA

HREC-7743-1
LMSC/HREC D162177

LOCKHEED MISSILES & SPACE COMPANY
HUNTSVILLE RESEARCH & ENGINEERING CENTER
HUNTSVILLE RESEARCH PARK
4800 BRADFORD DRIVE, HUNTSVILLE, ALABAMA

TRANSONIC FLOW IN A CONVERGING-DIVERGING NOZZLE

FINAL REPORT

Contract NAS7-743

by

R. J. Prozan

APPROVED: John W Benefield
J. W. Benefield, Supervisor
Propulsion Section

George D. Reny
G. D. Reny, Manager
Aeromechanics Dept.

George D. Reny for
J. S. Farrior
Resident Director

FOREWORD

This document presents the results of work performed by Lockheed Missiles & Space Company, Huntsville Research and Engineering Center, Huntsville, Alabama, under Contract NAS7-743, "Transonic Flow in a Converging-Diverging Nozzle."

The Contracting Agency is the National Aeronautics and Space Administration, Liquid Rocket Research and Technology Branch, Washington, D.C. The technical manager is Dr. R. F. Cuffel of the Jet Propulsion Laboratory, Pasadena, California.

SUMMARY

This document constitutes the final report of a study of steep angle nozzle inlets performed by Lockheed's Huntsville Research & Engineering Center under contract to the National Aeronautics and Space Administration. To be delivered with the final report is a computer program used to perform the calculations described herein.

Eight cases of interest to the National Aeronautics and Space Administration Jet Propulsion Laboratory, were analyzed and the results are presented in the main body of this report. These contours had steep inlets (75, 90 degrees) and very small nozzle wall radius of curvature to throat radius ratios (0.5, 0.25). The finite-difference techniques used in the analysis performed very well, particularly when the severity of the contours is considered.

Attached to the main body of this report are three appendixes. Appendix A discusses the theoretical approach to the finite difference solution reported herein. Appendix B is concerned with the computer program portion of the study. Appendix C contains the distribution list for this study.

The computer program described in Appendix B is considered to be extremely flexible, permitting several modes of operations for boundary conditions and grid structures. Many program control options are available for efficient utilization.

CONTENTS

NOMENCLATURE

M	Mach number
M^*	Mach number on wall at minimum area
m	radial station identifier
n	axial station identifier
q	velocity
R	gas constant
T	temperature
x, r	cylindrical coordinates
u, v	axial and radial velocity components in cylindrical coordinates system

Greek

α	defined in text
γ	ratio of specific heats
ρ	density
ξ, ψ	transformed coordinates

Subscripts and Superscripts

m	radial index
m_T	total number radial stations
n	axial index
n_s	minimum area axial station
n_T	total number axial stations
$'$	dimensional quantity

Section 1
INTRODUCTION

Transonic solutions for the converging-diverging region (throat) of rocket engines have occupied considerable attention in the scientific community. Contours in this region can greatly influence heat transfer and performance of the engines and, therefore, overall systems design. Analysis efforts in the past have centered around polynomial expansions of the potential function in the throat region. This approach, however, was limited until recently by throat radius of curvature to throat radius ratios that are generally exceeded in current designs. Moreover, these attempts did not consider the influence of inlet geometry for more than a short distance upstream of the physical throat.

Other attempts to describe these flow fields have utilized asymptotic time-dependent solutions to the finite difference equations of motion. Lockheed/Huntsville produced a program of this type which also considered non-isoenergetic flow. This program as well as programs produced by other organizations were plagued by stability problems inherent in the numerical analysis technique.

In an attempt to resolve the stability problem, Lockheed/Huntsville developed the Error Minimization technique. This numerical analysis approach has been successfully applied to transonic solutions with and without fuel striations. The unusual nozzle configurations of current interest to NASA/JPL, however, require a redevelopment of the coordinate system and the equations of motion in that system.

This study is divided into four tasks as follows:

1. Calculation of relatively steep inlet configurations which are within the capability of the existing program

2. Redevelopment of the equations of motion to consider inlet angles approaching 90 degrees

3. Execution of the computer program of Task 2, and

4. Documentation of the computer program and user's manual.

The first three items are discussed in the main body of this report and the last item is discussed in Appendix B.

Section 2
TECHNICAL DISCUSSION

The study effort identified in the Introduction of this report is divided, according to the Statement of Work, into three separate and distinct tasks (excluding documentation). In the interest of clarity, these tasks will be identified and discussed in chronological order.

TASK I – Statement

Utilizing the computer program described in Ref. 1, obtain the inviscid subsonic-transonic-supersonic flow field for four axisymmetric nozzle configurations. These are actually two nozzles each with different inlet configurations. The two nozzles have a steep convergent half-angle of approximately 75 deg. The divergent half angle is 15 deg and the throat radius is 0.8 in. One nozzle has a throat radius of curvature to throat radius ratio of 0.5 and the other 0.25. For each of these two nozzles the inlets will consist of:

- A conical inlet extending upstream to infinity.
- An axial flow inlet from a tube (contraction area ratio = 9.766) with transition to the convergent cone of the nozzle by means of a gradual turn which has a radius of curvature to throat radius ratio of 1.25.

To compute the flow field, an error-minimization technique is used to successively reduce the errors of the local finite-difference equations at the nodal points in a stretched Cartesian coordinate system.

TASK I – Discussion

The computer program described in Ref. 1 was not designed to handle the extremely steep inlet geometry which is the subject of this study. To provide interim results, however, this task was defined with a configuration of interest which could possibly be treated with the existing analysis.

Figure 1 depicts the Task I nozzle configurations. An attempt was made to analyze these nozzles with the analysis method of Ref. 1 but the computer program was not capable of treating these severe cases. The inability of the existing analysis to treat the Task I configurations, however, was not a serious setback because these same configurations were to be analyzed using an improved solution developed under Task II.

Task II – Statement

Reformulate the inviscid flow problem discussed in Task I to adequately treat very steep inlet angles (up to and including 90 deg). This may be accomplished by a transformation applied to the conservation equations such that grid lines in the transformed plane map into circular arcs which are normal to the centerline and normal to conical walls of the nozzle. This program will be written in ASA standard FORTRAN V language and will be operational on a Univac computer.

Task II – Discussion

Governing Equations: To simplify the subsequent analysis it is assumed that the working gas in the nozzles to be analyzed is an ideal perfect gas and that the flow is isoenergetic, inviscid, adiabatic and isentropic. Under these assumptions the conservation equations in cylindrical coordinates reduce to:

$$\frac{\partial(\rho'\mu')}{\partial x} + \frac{\partial(\rho' v')}{\partial r} + \frac{\rho' v'}{r} = 0 \qquad \text{(conservation of mass)} \qquad (1)$$

$$\frac{\partial v'}{\partial x} - \frac{\partial u'}{\partial r} = 0 \qquad \text{(condition of irrotationality)} \qquad (2)$$

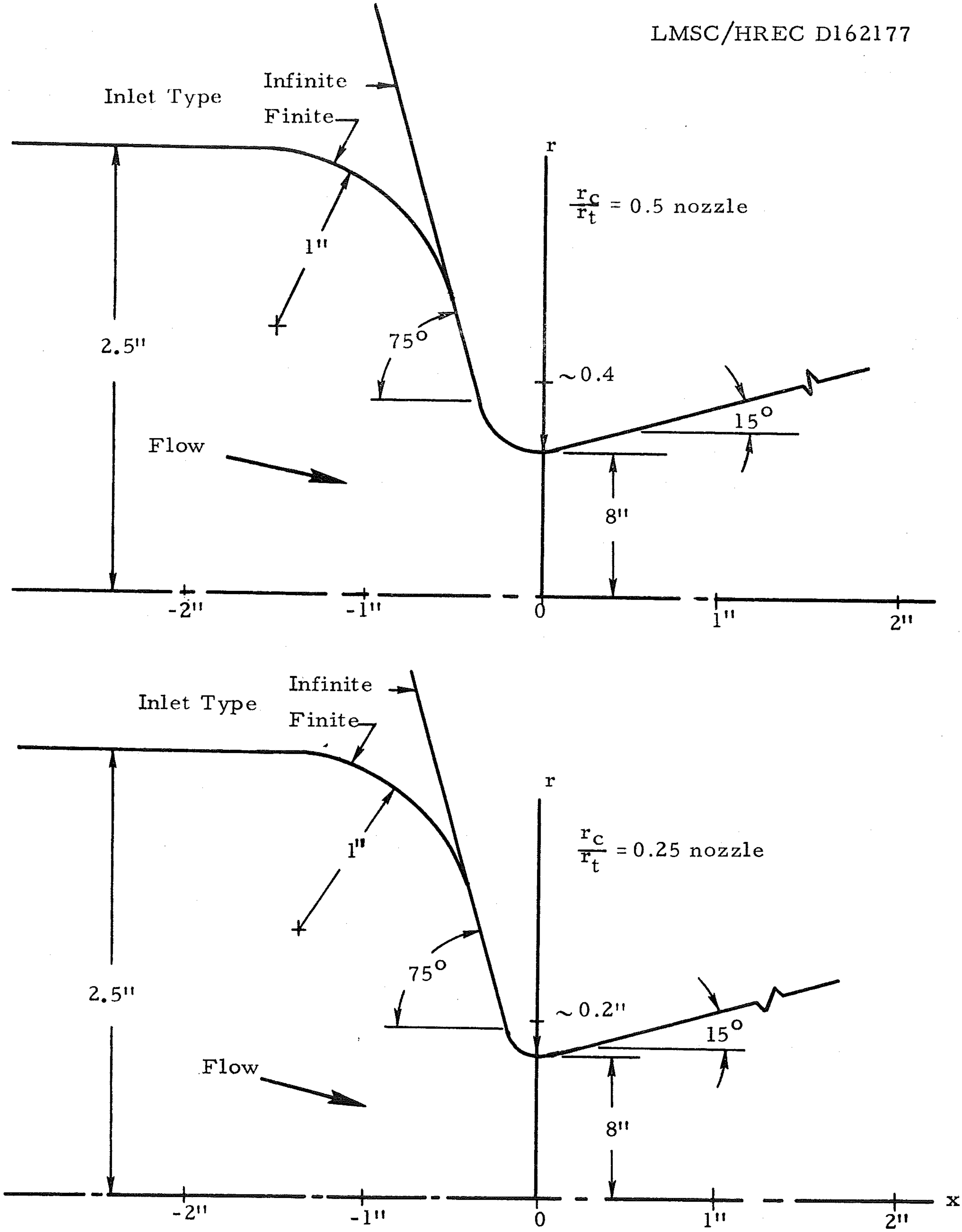

Fig. 1 - Task 1 Nozzle Geometries

From the above assumptions we may write

$$\frac{\rho'}{\rho_c} = \left(\frac{T'}{T_c}\right)^{1/(\gamma-1)} \tag{3}$$

where

$$\frac{T'}{T_c} = 1 - \frac{\gamma-1}{2\gamma R}\left(u'^2 + v'^2\right) \tag{4}$$

For the sake of convenience a change of variables is made;

$$\rho = \frac{\rho'}{\rho_c}; \quad T = \frac{T'}{T_c}; \quad u = \frac{u'}{\sqrt{\gamma R T_c}}; \quad v = \frac{v'}{\sqrt{\gamma R T_c}}$$

The above equations become

$$\frac{\partial(\rho u)}{\partial x} + \frac{\partial(\rho v)}{\partial r} + \frac{\rho v}{r} = 0 \tag{5a}$$

$$\frac{\partial v}{\partial x} - \frac{\partial u}{\partial r} = 0 \tag{5b}$$

$$\rho = T^{1/(\gamma-1)} \tag{5c}$$

$$T = 1 - \frac{\gamma-1}{2}\left(u^2 + v^2\right) \tag{5d}$$

Consider the transformation to the coordinate system;

$$x = x(\xi, \psi); \quad r = r(\xi, \psi)$$

Under such a transformation Eqs. (5a) and (5b) become

$$\frac{\partial r}{\partial \psi}\frac{\partial(\rho u)}{\partial \xi} - \frac{\partial x}{\partial \psi}\frac{\partial(\rho v)}{\partial \xi} + \frac{\partial x}{\partial \xi}\frac{\partial(\rho v)}{\partial \psi} - \frac{\partial r}{\partial \xi}\frac{\partial(\rho u)}{\partial \psi} + \frac{\alpha \rho v}{r} = 0 \tag{6a}$$

$$\frac{\partial r}{\partial \psi}\frac{\partial v}{\partial \xi} - \frac{\partial r}{\partial \xi}\frac{\partial v}{\partial \psi} + \frac{\partial x}{\partial \psi}\frac{\partial u}{\partial \xi} - \frac{\partial x}{\partial \xi}\frac{\partial u}{\partial \psi} = 0 \tag{6b}$$

where

$$\alpha = \frac{\partial r}{\partial \psi}\frac{\partial x}{\partial \xi} - \frac{\partial r}{\partial \xi}\frac{\partial x}{\partial \psi}$$

Figures 2 gives a schematic of the grid structure in the ξ, ψ plane (which is, of course, independent of the transformation). The grid is always centered and orthogonal even though the grid in the physical plane is not. The wall is always taken to correspond to $\psi = 1$ while the centerline is $\psi = 0$.

Recalling that $\rho = \rho(u, v)$ we may rewrite Eq. (6a)

$$r_\psi u_\xi - x_\psi v_\xi + x_\xi v_\psi - r_\xi u_\psi + \frac{\alpha v}{r}$$

$$-\frac{1}{T}\left\{\left[r_\psi u - x_\psi v\right]\left[u u_\xi + v v_\xi\right] + \left[x_\xi v - r_\xi u\right]\left[u u_\psi + v v_\psi\right]\right\} = 0 \tag{7}$$

Using the nomenclature of Fig. 3 and using central differences the finite-difference analogs to Eqs. (7) and (6b) are written:

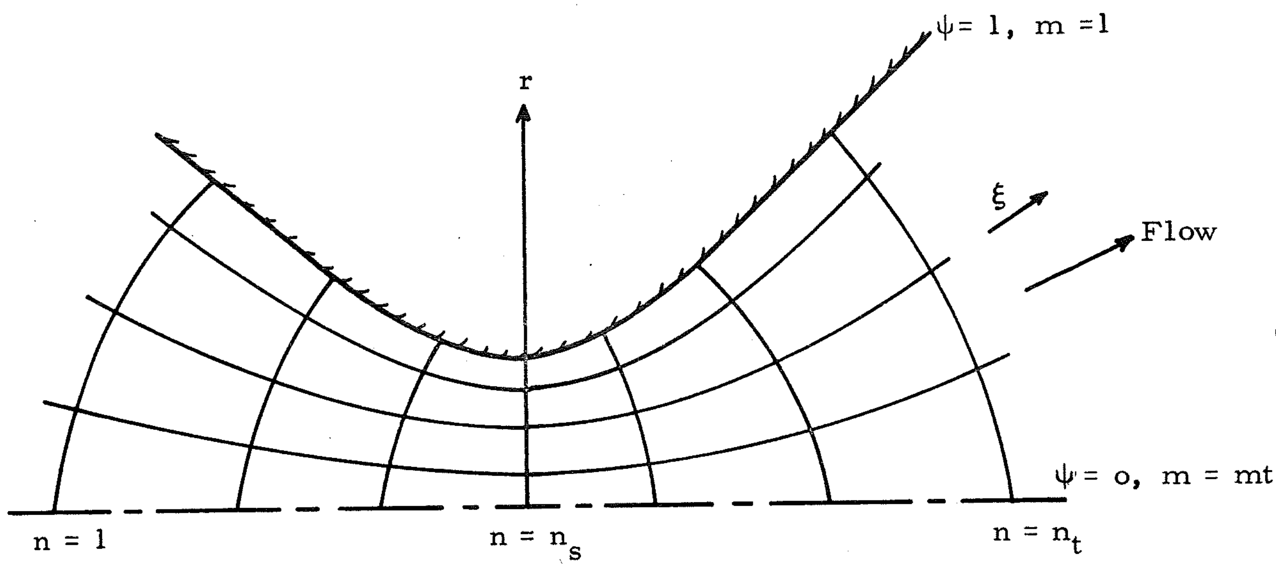

Fig. 2a - Grid Structure in m, x Plane

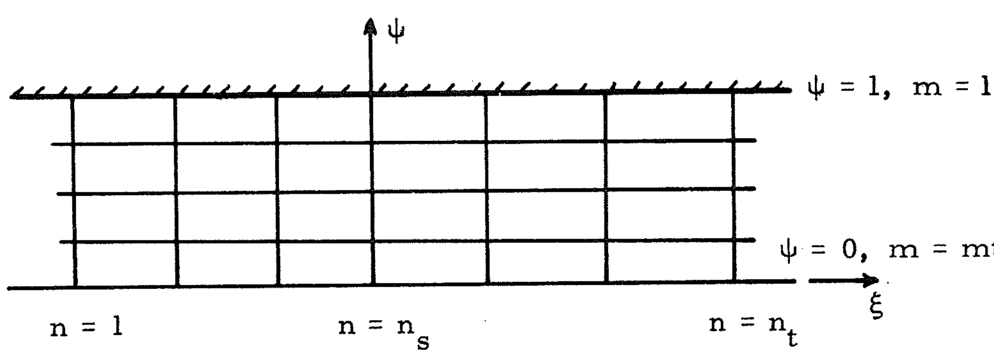

Fig. 2b - Grid Structure in ξ, ψ Plane

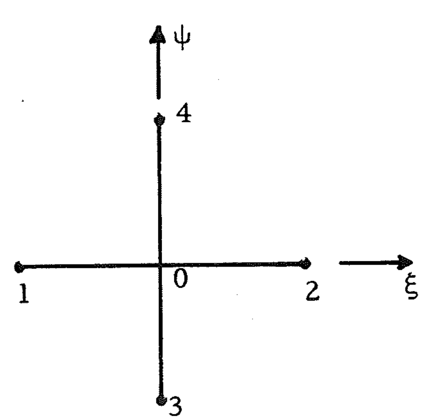

Fig. 3 - Finite Difference Grid

$$\bar{r}_\psi (u_2 - u_1) - \bar{x}_\psi (v_2 - v_1) + \bar{x}_\xi (v_4 - v_3) - \bar{r}_\xi (u_4 - u_3) + \frac{\bar{\alpha} v_o}{r_o}$$

$$- \frac{1}{T_o} \left\{ \left[\bar{r}_\psi u_o - \bar{x}_\psi v_o \right] \left[u_o (u_2 - u_1) + v_o (v_2 - v_1) \right] \right.$$

$$\left. + \left[\bar{x}_\xi v_o - \bar{r}_\xi u_o \right] \left[u_o (u_4 - u_3) + v_o (v_4 - v_3) \right] \right\} = 0 \qquad (8a)$$

$$\bar{r}_\psi (v_2 - v_1) - \bar{r}_\xi (v_4 - v_3) + \bar{x}_\psi (u_2 - u_1) - \bar{x}_\xi (u_4 - u_3) = 0 \qquad (8b)$$

where

$$\bar{r}_\psi = r_4 - r_3; \qquad \bar{x}_\psi = x_4 - x_3$$

$$\bar{r}_\xi = r_2 - r_1; \qquad \bar{x}_\xi = x_2 - x_1$$

and where

$$\bar{\alpha} = \bar{r}_\psi \bar{x}_\xi - \bar{r}_\xi \bar{x}_\psi$$

Equations (8a) and (8b) must be satisfied for every grid point, (at least every interior grid point) in the field.

To complete the solution, equations governing the behavior of the wall, centerline, inlet and outlet points are needed. Unfortunately these equations are not currently embodied in the steady state theory, and approximate relations must be used.

The upper wall condition is approximated by a linear extrapolation of the square of speed from adjacent points;

$$q^2\Big|_{\psi=1} = 2q^2\Big|_{1-\Delta\psi} - q^2\Big|_{1-2\Delta\psi} \tag{9a}$$

and is used in conjunction with the tangency conditions,

$$v\big|_{\psi=1} = \tan\theta_w \, u\big|_{\psi=1} \tag{9b}$$

For the centerline, use is made of symmetry to yield (second order extrapolation);

$$u\big|_{\psi=0} = \frac{1}{3}\left\{4u\big|_{\Delta\psi} - u\big|_{2\Delta\psi}\right\} \tag{9c}$$

and the tangency condition is given by

$$v\big|_{\psi=0} = 0 \tag{9d}$$

The inlet and outlet grid station will be discussed later.

Numerical Solution of Governing Equations: The previously derived relations must now be satisfied over the entire flow field. It should be noted that the governing equations are now nonlinear algebraic equations where u, v are independent variables rather than the original partial differential equations in which the spatial coordinates were independent.

The Error Minimization technique, first reported in Ref. 1 is used to effect the numerical solution. A discussion of this technique with application to this problem may be found in Appendix A, while a discussion of the computer program generated in this study may be found in Appendix B.

Task III – Statement

Utilizing the computer program developed under Task II, obtain the subsonic-transonic-supersonic solutions for eight nozzle configurations. Actually there are four nozzles, each with two different inlets. Two of the nozzles are the same as described in Task I. The other two differ only by the convergent half angle which is 90 deg instead of 75 deg. With each of these four nozzles the inlets described in Task I or their equivalents will be used. Figure 4 illustrates the additional nozzle configurations to be analyzed.

In general, as expected, the dominant parameter in these configurations is the radius ratio (radius of curvature of the throat/radius of the throat). Accordingly the configurations with identical radius ratios are presented together. Figure 5 gives the computer program results for the 0.5 radius ratio nozzles while Fig. 6 gives the results for the 0.25 radius ratio nozzles. Plotted in these figures are the wall and centerline Mach number distributions.

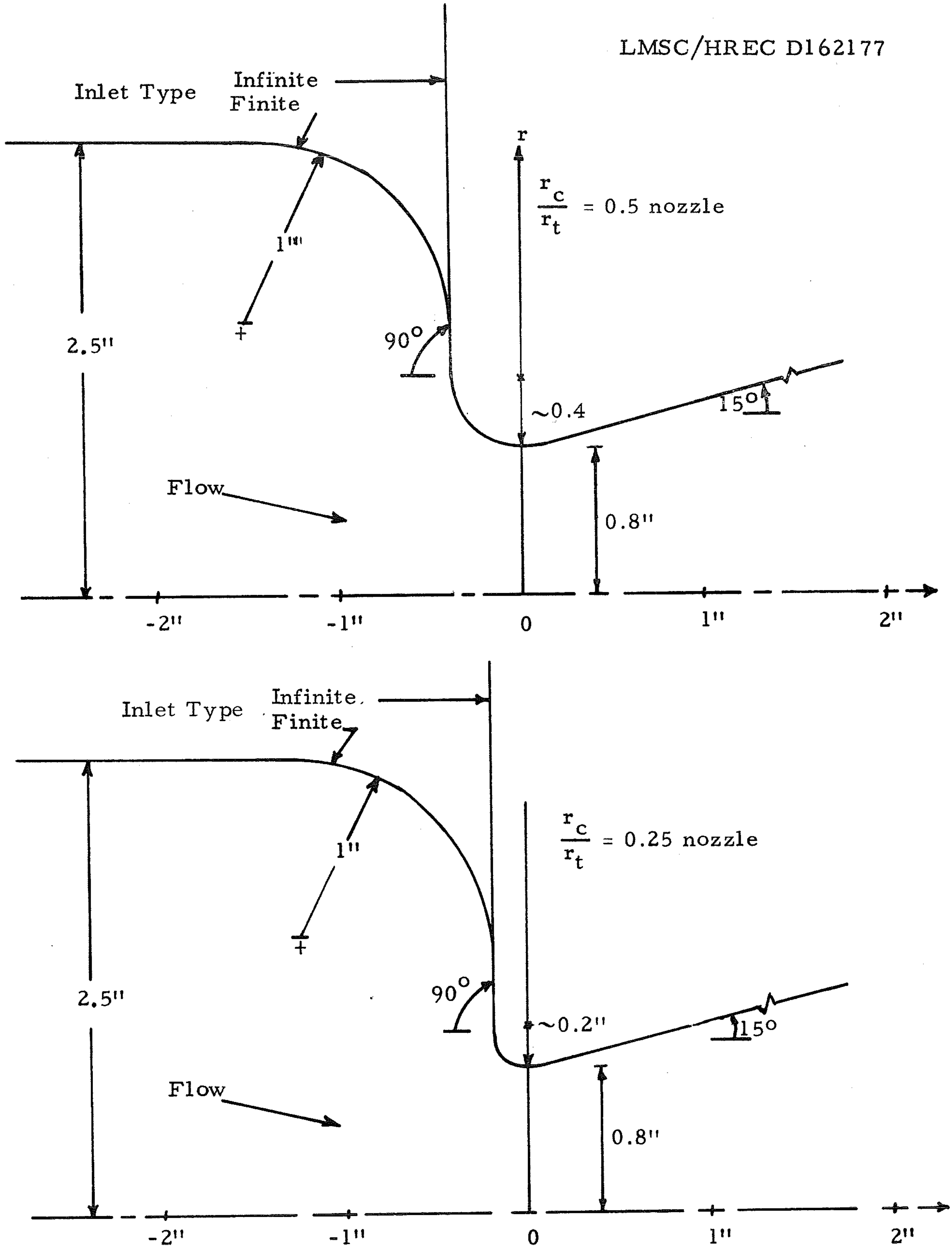

Fig. 4 - Task 2 Additional Nozzle Geometries

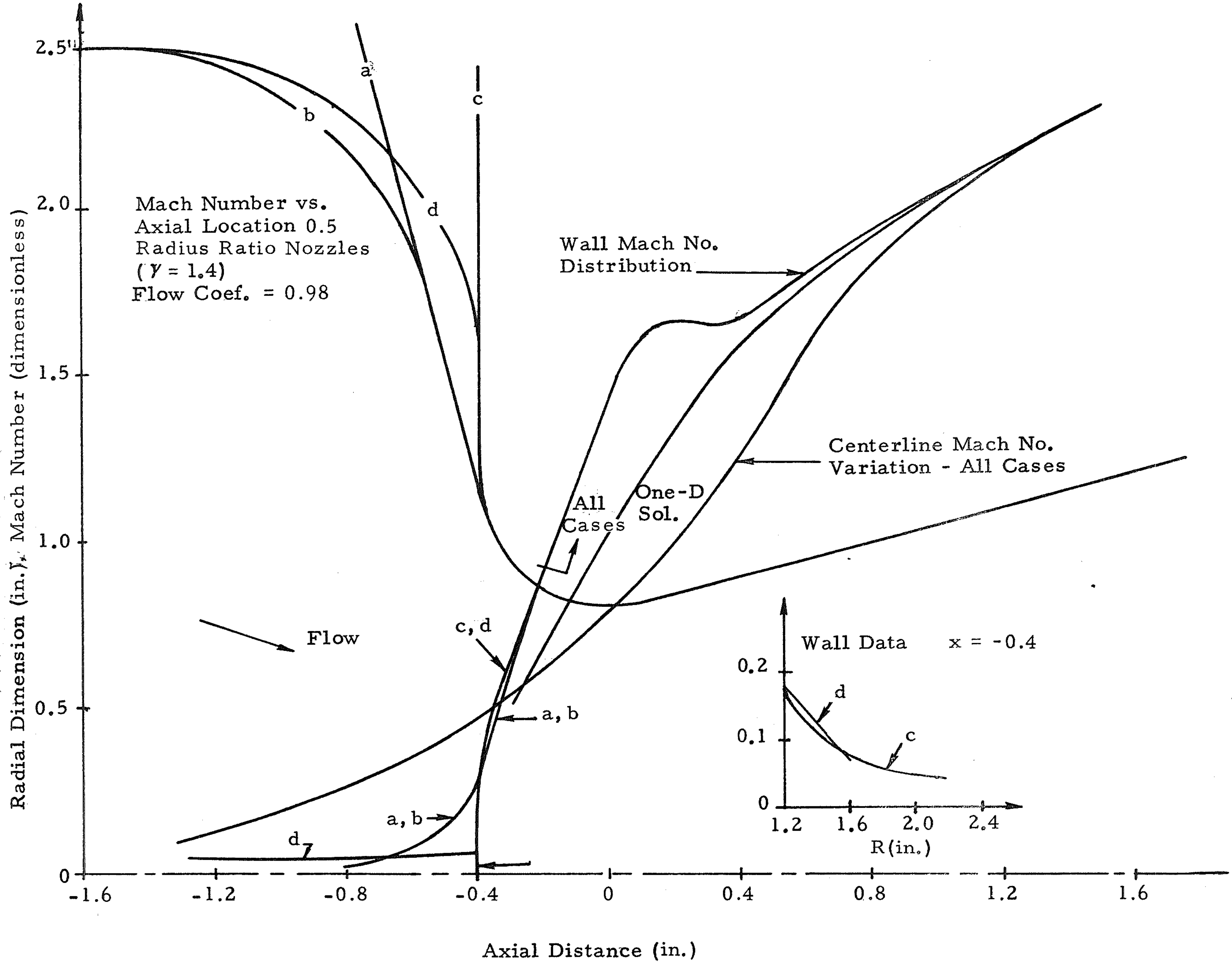

Fig. 5 - 0.5 Radius Ratio Nozzle Solutions

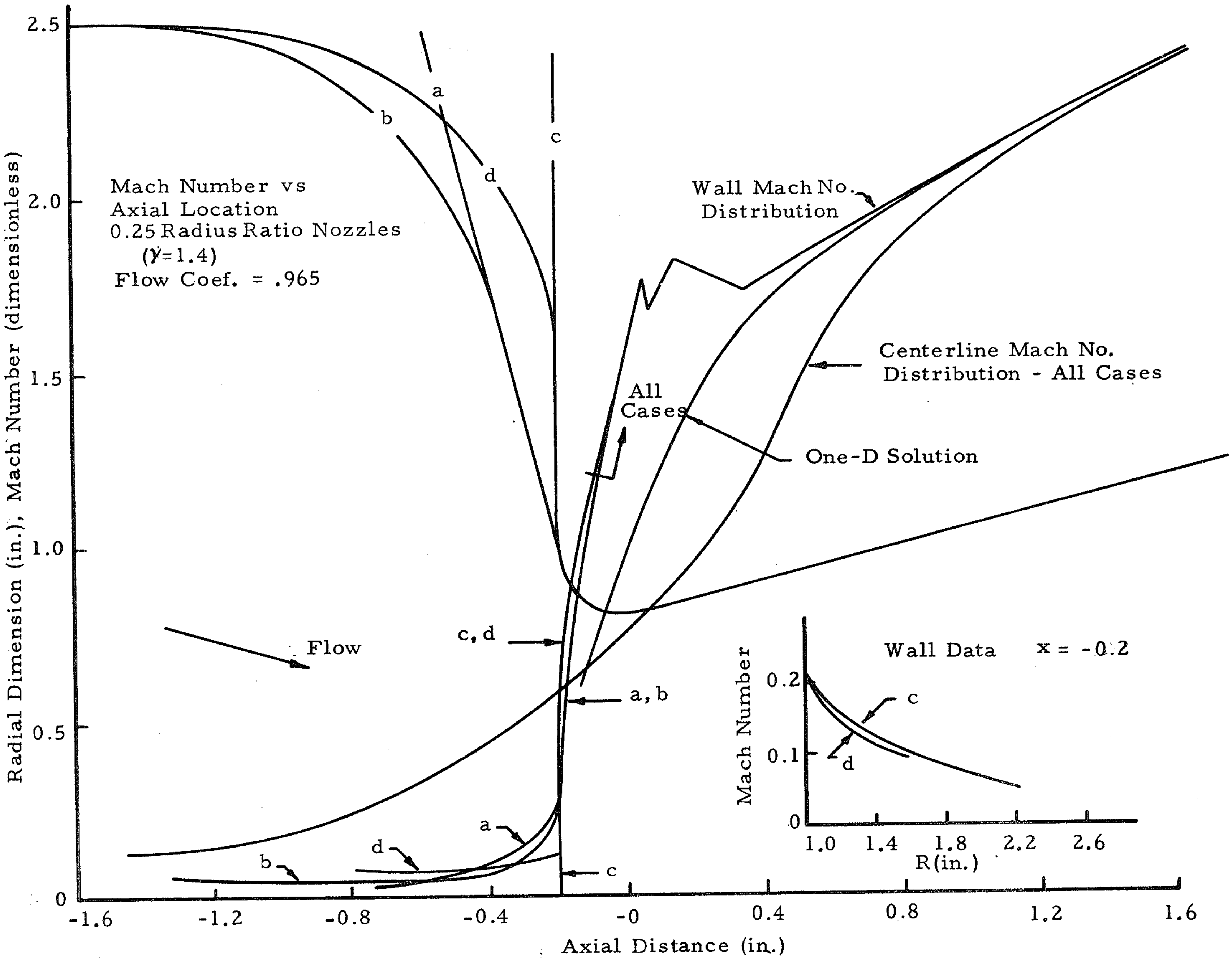

Fig. 6 – 0.25 Radius Ratio Nozzle Solutions

Section 3
RESULTS

The most striking result is, of course, that the Mach number distributions are virtually identical on the wall for those regions in which the contour is common to all cases on both the 0.5-radius-ratio and 0.25-radius-ratio nozzles. Although the scaling or weighting techniques described in Appendix A would tend to produce such a result this effect cannot be rationalized solely on that basis.

It can be concluded that the throat is indeed the boundary condition and that the inlet and outlet do indeed respond to the throat influence but only within certain bounds, i.e., a throat distribution which requires an impossible inlet distribution is prevented. As such the throat is not an absolute boundary condition. This conclusion is supported by the fact that in an elliptic region there is a mutual interplay or exchange of information.

Figure 7 illustrates the effect of radius ratio and inlet angle on the throat flow angle distribution for the reservoir inflow cases. The corresponding axial inflow results are again virtually identical. As can be seen, a noticeable alteration of the flow angle distribution occurs due to an inlet angle change from 75 deg to 90 deg for the 0.25-radius-ratio case. This effect is barely perceptible on the 0.5-radius-ratio case.

It also should be noted (Fig.6) that there exists a tendency to produce waves at the juncture of the throat circle and the exit cone. Whether this is caused by the large velocity gradients in this region or by the nozzle envelope shock wave has not yet been determined. Attempts to introduce smoothing utilizing the second derivatives of the velocity components (similar to pseudo-viscous terms in unsteady asymptotic analyses) have been only moderately successful.

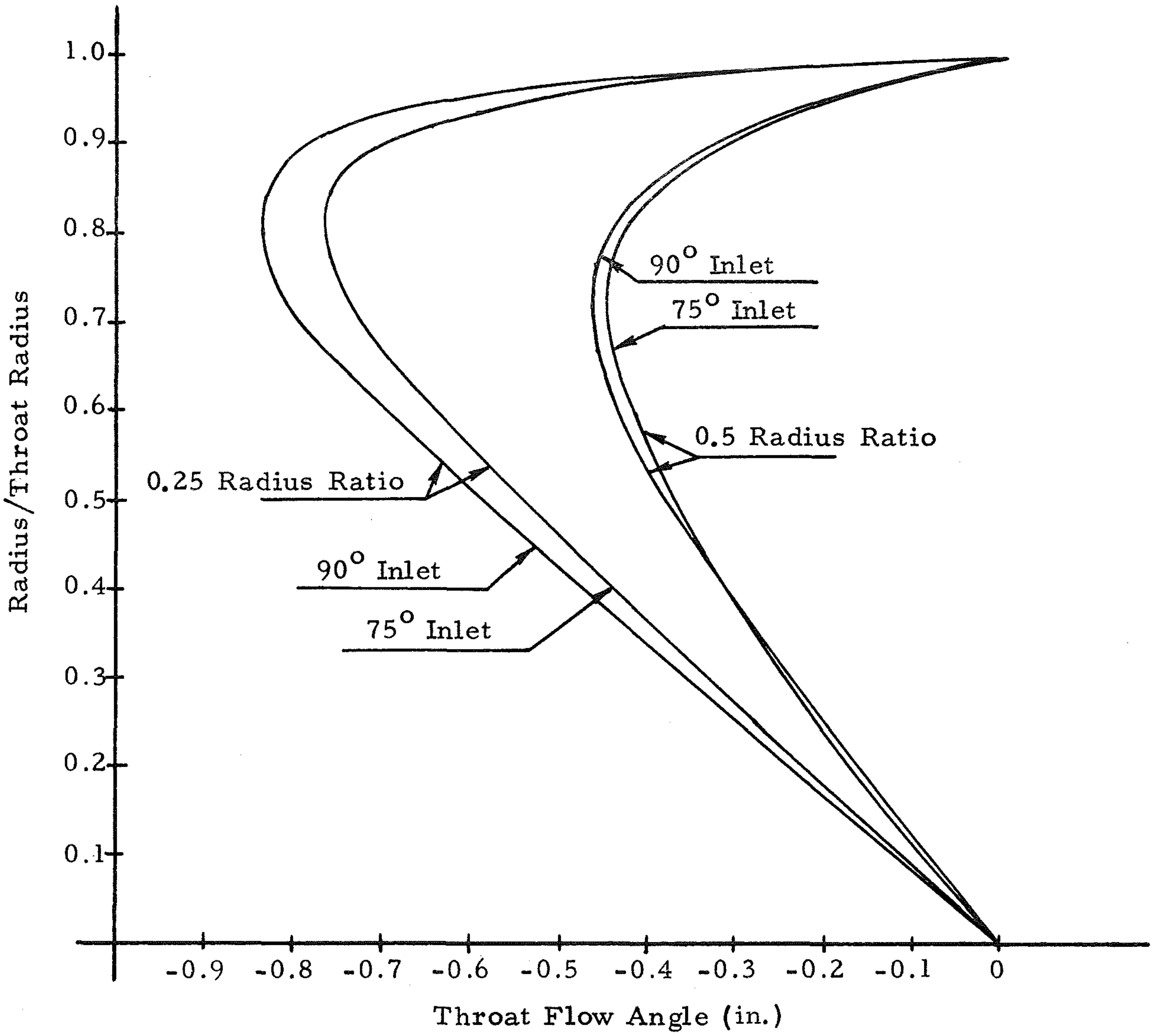

Fig. 7 - Throat Flow Angle vs Radial Position for Reservoir Inflow Cases

Conclusions

The accuracy of the techniques used in this study have been verified for moderate inlet angles and throat radius ratios by Ref. 1. It is reasonable to expect that the generalization of the grid distribution system will, with judicious use enhance rather than detract from the accuracy. It is further to be expected that the accuracy of the results will improve with a finer grid system than used in the example calculations. The predictions presented in this report are consistent and reasonable. The precision of the results must be determined by comparison with experimental data.

Future Work

It is felt that this study has been a demonstration of the power of finite-difference techniques. Unfortunately, the science of numerical methods is imperfect. The conservation equations adequately describe the interior of the flow but boundary conditions are ill defined. Studies currently in progress at Lockheed/Huntsville inevitably lead to the conclusion that the major stumbling block in finite-difference analysis is the adequate knowledge and treatment of boundary conditions.

For numerical techniques to truly come into their own it is imperative that the proper boundary condition relationships be found. It is suggested that studies investigating these boundary conditions are a necessary next step in the pursuit of numerical solutions to complex flow fields.

REFERENCE

1. Prozan, R. J. and D. E. Kooker, "A Transonic Nozzle Solution Using the Error Minimization Technique," LMSC/HREC D148622, Lockheed Missiles & Space Company, Huntsville, Ala., 1969.

Appendix A

THE ERROR MINIMIZATION TECHNIQUES AS APPLIED TO TRANSONIC FLOW IN A CONVERGING-DIVERGING DUCT

NOMENCLATURE

A, B, C, D	defined in text
G	solution merit function
g	local contribution to total error
$\bar{\ell}$	unit vector
n_s	minimum area axial station
q	velocity
$\bar{s}$	solution vector
T	temperature
u, v	velocity components in cylindrical systems
x, r	cylindrical coordinates
$\leftarrow$	replace operation

Greek

γ	ratio of specific heats
δ	step modifier
ϵ	residual or error
ν	any independent variable
ξ, ψ	transformed system coordinates
Γ	scale function

Subscripts and Superscripts

m	radial station index
m_T	maximum radial station index
n	axial station index
n_T	maximum axial station

DISCUSSION

A.1 INTERIOR POINTS

In the main body of this report is was shown that the finite-difference analogs to the conservation of mass and the irrotationality condition were:

$$\bar{r}_\psi (u_2 - u_1) - \bar{x}_\psi (v_2 - v_1) + \bar{x}_\xi (v_4 - v_3) - \bar{r}_\xi (u_4 - u_3) + \bar{\alpha} \frac{v_0}{r_0}$$

$$- \frac{1}{T_0} \Big\{ \left[\bar{r}_\psi u_0 - \bar{x}_\psi v_0\right]\left[u_0 (u_2 - u_1) + v_0 (v_2 - v_1)\right]$$

$$+ \left[\bar{x}_\xi v_0 - \bar{r}_\xi u_0\right]\left[u_0 (u_4 - u_3) + v_0 (v_4 - v_3)\right]\Big\} = 0 \qquad \text{(A.1)}$$

$$\bar{r}_\psi (v_2 - v_1) - \bar{r}_\xi (v_4 - v_3) + \bar{x}_\psi (u_2 - u_1) - \bar{x}_\xi (u_4 - u_3) = 0 \qquad \text{(A.2)}$$

where

$$\bar{r}_\psi = r_4 - r_3 \quad ; \quad \bar{x}_\psi = x_4 - x_3$$

$$\bar{r}_\xi = r_2 - r_1 \quad ; \quad \bar{x}_\xi = x_2 - x_1$$

$$\bar{\alpha} = \bar{r}_\psi \bar{x}_\xi - \bar{r}_\xi \bar{x}_\psi$$

For an arbitrary initial estimate of the flow conditions equations (1) and (2) will be in error at each interior grid point in the field. If an interior point is described by subscripts m,n then the errors in Eqs. (A.1) and (A.2) are $\varepsilon_{1_{m,n}}$ and $\varepsilon_{2_{m,n}}$, respectively.

The problem reduces to one of driving the errors at every point in the flow field to zero (or at least reducing them substantially).

Now let

$$g_{m,n} = \varepsilon_{1\,m,n}^{2} + \varepsilon_{2\,m,n}^{2} \tag{A.3}$$

Obviously $g_{m,n}$ is positive definite and is zero only when the errors are zero. Further let

$$G = \sum_{n=2}^{n_T-1} \sum_{m=2}^{m_T-1} g_{m,n} \tag{A.4}$$

Again if $g_{m,n}$ is zero for every m,n then G is a positive definite function which has an absolute minimum at the desired solution point.

From calculus

$$dG = \nabla G \cdot d\bar{s} = \nabla G \cdot \bar{e}_s \, ds$$

where ds is an infinitesimal displacement along the unit vector $\bar{e}_s$. For any given displacement ds, dG is a maximum when

$$\frac{\nabla G}{|\nabla G|} \cdot \bar{e}_s = 1 \quad ; \quad \frac{\nabla G}{|\nabla G|} = \bar{e}_s$$

then

$$dG = \nabla G \cdot \frac{\nabla G}{|\nabla G|} \, ds = |\nabla G| \, ds$$

but the largest possible change in G is

$$dG \cong G^{(\ell+1)} - G^{(\ell)} = -G^{(\ell)}$$

if the minimum was found on the next step then

$$dS = \frac{-G}{|\nabla G|}$$

while

$$d\bar{S} = \bar{e}_s ds = \frac{-G\nabla G}{|\nabla G|^2}$$

of course, $d\bar{S}$ is the change in the independent vector, so that

$$\bar{S}^{(\ell+1)} = \bar{S}^{(\ell)} - \left(\frac{G\nabla G}{|\nabla G|^2}\right)^{(\ell)}$$

The above expression is a first-order multivariable counterpart of the familar Newton-Raphson recursion formula. It is quite possible that the value of $G^{(\ell+1)}$ may be greater than $G^{(\ell)}$. It may be recalled that the step length was calculated under the optimistic assumption that the next value of G would be zero. It is in fact immaterial to the technique how long a step is taken as long as $G^{(\ell+1)}$ is less than $G^{(\ell)}$. A step modifier is therefore added to the above recursion formula to achieve the final form used in the error minimization technique.

$$\bar{S}^{(\ell+1)} = \bar{S}^{(\ell)} - \left(\frac{G\delta}{|\nabla G|^2}\right)^{(\ell)} \nabla G^{(\ell)} \qquad \text{(A.5)}$$

In the computer program discussed in Appendix B the initial value of δ was chosen as unity and each time that a new value of G was calculated that was greater than the previous value, δ was set to 75% of its previous value. No large amount of scientific thought went into this choice, and experimentation and investigation of the behavior of δ might well significantly reduce the computation time.

Repetitive use of Eqs. (A.1) and (A.2) over the entire flow field allow the evaluation of the merit function G for the current relaxation step. In order to apply Eq. (A.5), however, to alter the independent vector, the gradient of G must be calculated. Now

$$\frac{\partial G}{\partial u_{i,j}} = \sum_{n=2}^{n_T-1} \sum_{m=2}^{m_T-1} \frac{\partial g_{m,n}}{\partial u_{i,j}} \qquad (i=1,n_T \; ; \; j=1,m_T)$$

Because of the five point influence this reduces to

$$\frac{\partial G}{\partial u_{m,n}} = \frac{\partial g_{m+1,n}}{\partial u_{m,n}} + \frac{\partial g_{m-1,n}}{\partial u_{m,n}} + \frac{\partial g_{m,n}}{\partial u_{m,n}} + \frac{\partial g_{m,n+1}}{\partial u_{m,n}} + \frac{\partial g_{m,n-1}}{\partial u_{m,n}} \tag{A.6}$$

In the actual calculation, it becomes very inefficient to calculate the above expression directly. It is however very easy to calculate the following terms while at point m,n

$$\frac{\partial g_{m,n}}{\partial u_{m+1,n}} \; ; \; \frac{\partial g_{m,n}}{\partial u_{m-1,n}} \; ; \; \frac{\partial g_{m,n}}{\partial u_{m,n}} \; ; \; \frac{\partial g_{m,n}}{\partial u_{m,n+1}} \; ; \; \frac{\partial g_{m,n}}{\partial u_{m,n-1}}$$

where $(m+1,n)$, $(m-1,n)$, (m,n), $(m,n+1)$, $(m,n-1)$ are identified as points 3, 4, 0, 2, 1 in Eqs. (A.1) and (A.2). It also can be seen that

$$\frac{\partial g_0}{\partial \nu} = 2\varepsilon_{1(0)} \frac{\partial \varepsilon_{1(0)}}{\partial \nu} + 2\varepsilon_{2(0)} \frac{\partial \varepsilon_{2(0)}}{\partial \nu}$$

where ν is any variable in the system.

Equations (A.1) and (A.2) may then be differentiated with respect to the velocity components. For simplicity Eq. (A.1) is rewritten

$$\bar{h}_\psi (u_2 - u_1) - \bar{x}_\psi (v_2 - v_1) + \bar{x}_\xi (v_4 - v_3) - \bar{h}_\xi (u_4 - u_3) + \frac{\bar{\alpha} v_0}{h_0}$$

$$- \frac{1}{T_0} \left\{ AB + CD \right\}$$

where

$$A = \bar{h}_\psi u_0 - \bar{x}_\psi v_0 \quad ; \quad B = u_0 (u_2 - u_1) + v_0 (v_2 - v_1)$$

$$C = \bar{x}_\xi v_0 - \bar{h}_\xi u_0 \quad ; \quad D = u_0 (u_4 - u_3) + v_0 (v_4 - v_3)$$

Then;

$$\frac{\partial \varepsilon_{1(0)}}{\partial u_0} = \frac{-1}{T_0} \left[(\gamma - 1) \frac{u_0}{T_0} (AB + CD) + \bar{h}_\psi B + (u_2 - u_1) A - \bar{h}_\xi D + (u_4 - u_3) C \right] \tag{A.7a}$$

$$\frac{\partial \varepsilon_{1(0)}}{\partial v_0} = \frac{\bar{\alpha}}{h_0} - \frac{1}{T_0} \left[(\gamma - 1) \frac{v_0}{T_0} (AB + CD) - \bar{x}_\psi B + (v_2 - v_1) A + \bar{x}_\xi D + (v_4 - v_3) C \right] \tag{A.7b}$$

$$\frac{\partial \varepsilon_{2(0)}}{\partial u_0} = \frac{\partial \varepsilon_{2(0)}}{\partial v_0} = 0 \tag{A.7c}$$

$$\frac{\partial \varepsilon_{1(0)}}{\partial u_1} = -\bar{h}_\psi + \frac{u_0 A}{T_0} = -\frac{\partial \varepsilon_{1(0)}}{\partial u_2} \tag{A.7d}$$

$$\frac{\partial \varepsilon_{1(0)}}{\partial v_1} = \bar{x}_\psi + \frac{v_0 A}{T_0} = -\frac{\partial \varepsilon_{1(0)}}{\partial v_2} \tag{A.7e}$$

$$\frac{\partial \varepsilon_{2(0)}}{\partial u_1} = -\bar{x}_\psi = -\frac{\partial \varepsilon_{2(0)}}{\partial u_2} \tag{A.7f}$$

$$\frac{\partial \varepsilon_{2(0)}}{\partial v_1} = -\bar{h}_\psi = -\frac{\partial \varepsilon_{2(0)}}{\partial v_2} \tag{A.7g}$$

$$\frac{\partial \varepsilon_{1(0)}}{\partial u_3} = \bar{h}_\xi + \frac{u_0}{T_0} C = -\frac{\partial \varepsilon_{1(0)}}{\partial u_4} \tag{A.7h}$$

$$\frac{\partial \varepsilon_{1(0)}}{\partial v_3} = -\bar{x}_\xi + \frac{\bar{v}_0}{T_0} C = -\frac{\partial \varepsilon_{1(0)}}{\partial v_4} \tag{A.7i}$$

$$\frac{\partial \varepsilon_{2(0)}}{\partial u_3} = \bar{x}_\xi = -\frac{\partial \varepsilon_{2(0)}}{\partial u_4} \tag{A.7j}$$

$$\frac{\partial \varepsilon_{2(0)}}{\partial v_3} = \bar{r}_\xi = -\frac{\partial \varepsilon_{2(0)}}{\partial v_4} \tag{A.7k}$$

As a sweep is made through all interior points the gradient is constructed by summing the contributions in the appropriate fashion, i.e.,

$$\frac{\partial G}{\partial u_{m,n}} \longleftarrow \frac{\partial G}{\partial u_{m,n}} + \frac{\partial g_{i,j}}{\partial u_{m,n}}$$

$$\frac{\partial G}{\partial v_{m,n}} \longleftarrow \frac{\partial G}{\partial v_{m,n}} + \frac{\partial g_{i,j}}{\partial v_{m,n}}$$

After the sweep of the entire flow field has been completed, the gradient vector will have been properly formed. Any confusion concerning this process will be clarified by examining subroutine EMT in Appendix B.

A.2 BOUNDARY POINTS

As discussed in the main body of the report, an approximation to the wall boundary condition is

$$q^2_{1,n} = 2q^2_{2,n} - q^2_{3,n} \tag{A.8}$$

where points 1, 2, 3 correspond to $\psi = 1$, $1-\Delta\psi$, $1-2\Delta\psi$ respectively. Now

$$q^2 = u^2 + v^2$$

so that the differential of Eq. (A.8) is

$$2u_{1,n}\, du_{1,n} + 2v_{1,n}\, dv_{1,n} = 4\left(u_{2,n}\, du_{2,n} + v_{2,n}\, dv_{2,n}\right)$$

$$- 2\left(u_{3,n}\, du_{3,n} + v_{3,n}\, dv_{3,n}\right)$$

but

$$v_{1,n} = \tan\theta_w\, u_{1,n}$$

and

$$dv_{1,n} = \tan\theta_w\, du_{1,n}$$

so that

$$u_{1,n}\, du_{1,n}\left(1 + \tan^2\theta_w\right) = 2\left(u_{2,n}\, du_{2,n} + v_{2,n}\, dv_{2,n}\right)$$

$$-\left(u_{3,n}\, du_{3,n} + v_{3,n}\, dv_{3,n}\right)$$

It can be seen from Eq. (A.5) that the change in each independent variable can be found from the recursion formula. Therefore

$$\frac{\partial G}{\partial u_{1,n}} = \left\{2\left(u_{2,n}\frac{\partial G}{\partial u_{2,n}} + v_{2,n}\frac{\partial G}{\partial v_{2,n}}\right) - \left(u_{3,n}\frac{\partial G}{\partial u_{3,n}} + v_{3,n}\frac{\partial G}{\partial v_{3,n}}\right)\right\} \Big/ \left(1 + \tan^2\theta_w\right) u_{1,n} \tag{A.9}$$

In order to retain the proper tangency relationship

$$\frac{\partial G}{\partial v_{1,n}} = \tan\theta_w \frac{\partial G}{\partial u_{1,n}} \tag{A.10}$$

Similarly, the centerline conditions yield

$$\frac{\partial G}{\partial u_{1,n}} = \frac{1}{3}\left(4\frac{\partial G}{\partial u_{2,n}} - \frac{\partial G}{\partial u_{3,n}}\right) \tag{A.11}$$

$$\frac{\partial G}{\partial r_{1,n}} = 0 \qquad \text{(A.12)}$$

where points 1, 2, 3 correspond to $\psi = 0$, $\Delta\psi$, $2\Delta\psi$ respectively.

It may be noticed that components of the gradient surface are calculated at all interior points plus all surrounding or non-interior points. Equations (A.9) through (A.12) ignored or destroyed this information at the wall and centerline. At the inlet and outlet however use is made of this information to alter the variables at these stations such that the function G is minimized. This is consistent with the assumption that these surfaces are not boundary conditions.

Equations (A.1) and (A.2) are not altered if they are multiplied by some scale factor. In this problem it is advantageous to multiply the equations by a scale factor which emphasizes the throat. The scale used was

$$I_n = e^{-\sqrt{|(n-n_s)|}}$$

where n_s is the throat station. The local error terms are redefined

$$\varepsilon'_{1\,m,n} = I_n\,\varepsilon_{1\,m,n} \quad ; \quad \varepsilon'_{2\,m,n} = I_n\,\varepsilon_{2\,m,n}$$

and all pertinent equations are altered appropriately. It is felt that the proper formulations currently under investigation should automatically provide this type of scaling or emphasis of the throat. For the time being the above approach is justifiable from the numerical viewpoint. The scaling tends to sacrifice the end regions in order to improve the throat region. It is this flow of information away from the throat which implicitly causes the throat to act as the boundary condition.

Using the governing equations and process described above the nozzle solution described in Appendix B yields the results shown in Fig. (A.1) for the 90 deg inlet, 0.25 radius ratio, reservoir inflow case. It can be seen that the results are wavy in the supersonic region. The reason for this effect is not known and is certainly not a physical phenomenon. The problem may be due to the rapid turning of the flow through the low transonic being suddenly restricted to flowing parallel to the conical exit. This recompression effect due to the discontinuity in second derivatives is well known and gives rise to a nozzle shock wave.

In any event a method has been incorporated into the solution to smooth the results. This is a user-selected option and is generally not employed until the unsmoothed relaxation equations have approached a final solution. In this way it is possible to calculate the unsmoothed solution as well as the smoothed. The smoothing is accomplished by introducing error terms based on the second derivative;

$$
\begin{aligned}
\varepsilon_{3\,m,n} &= u_2 + u_1 - 2u_0 \\
\varepsilon_{4\,m,n} &= v_2 + v_1 - 2v_0 \\
\varepsilon_{5\,m,n} &= u_4 + u_3 - 2u_0 \\
\varepsilon_{6\,m,n} &= v_4 + v_3 - 2v_0
\end{aligned}
\tag{A.13}
$$

Driving, or attempting to drive, the second derivative to zero implies that the functions must be linear, certainly an unsatisfactory situation. The magnitude of these terms is kept small, however, so that the smoothing does not introduce errors in the differential equation solution. Scaling Eqs. (A.13) by 0.03 I yields the second set of results on Figs. A.1 and A.2.

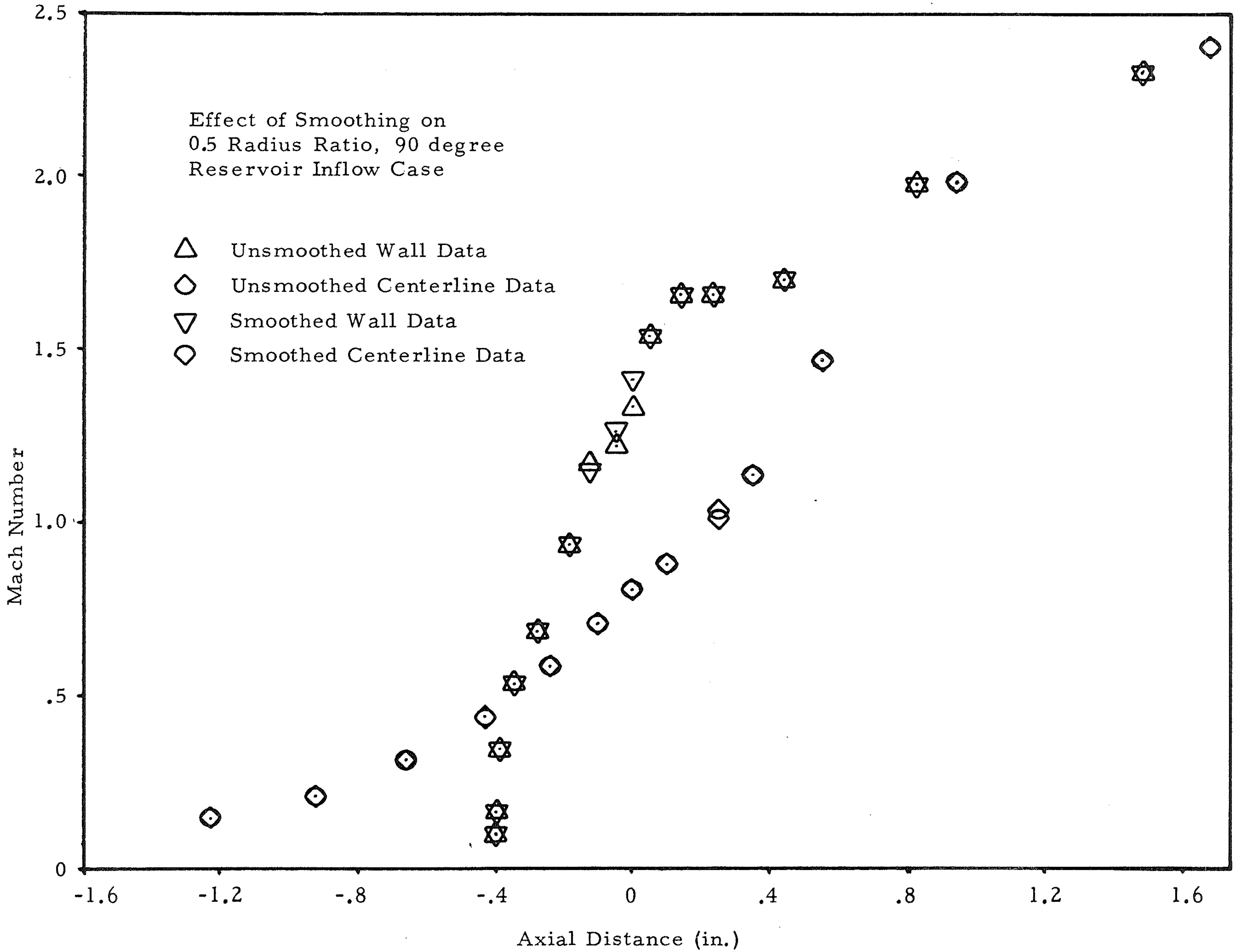

Fig. A-1 — Effects of Smoothing on .5 Radius Ratio Solution

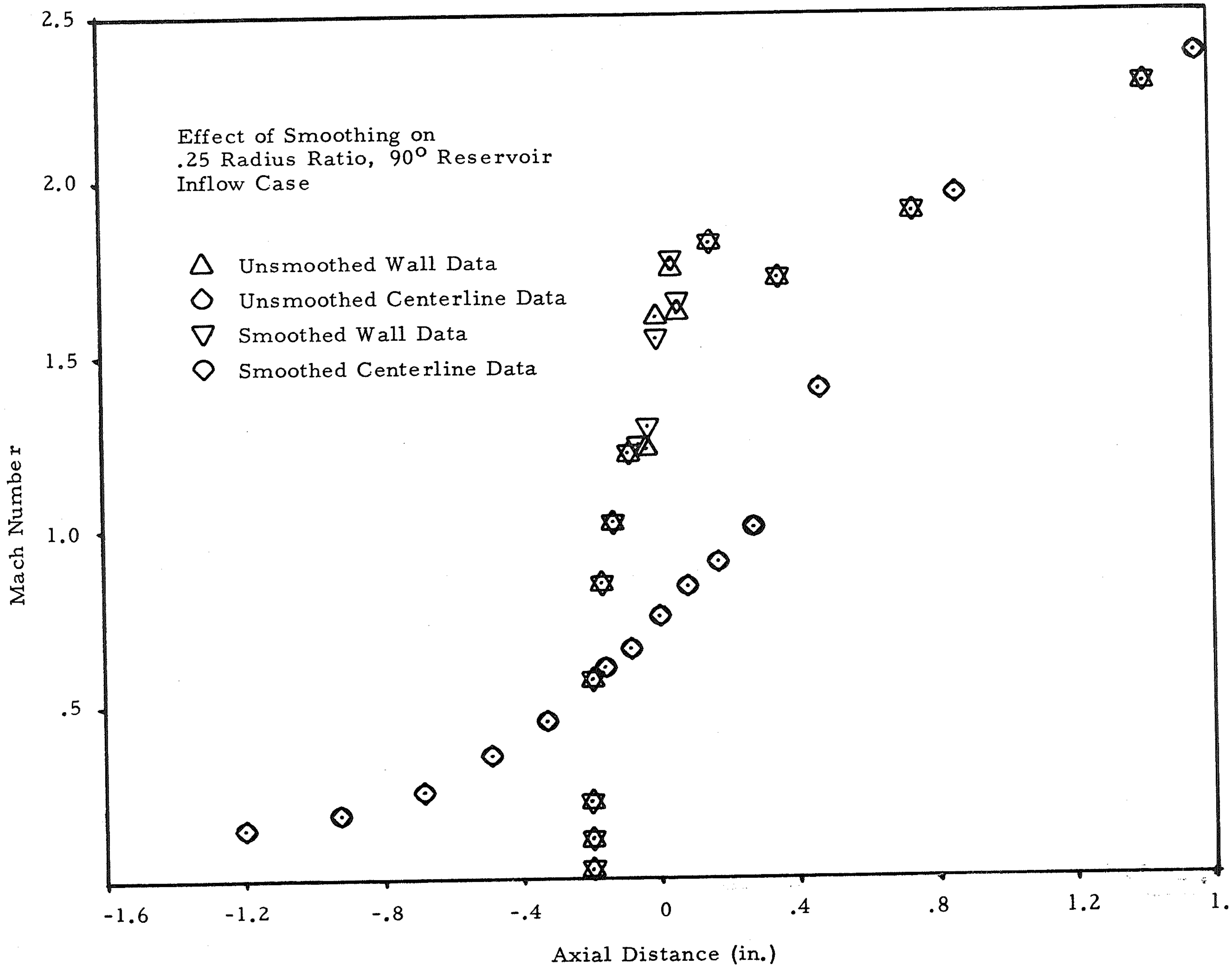

Fig. A-2 – Effect of Smoothing on .25 Radius Ratio Solutions

A.3 CONCLUSION

The Error Minimization analysis is straightforward, simple and rapid. It is certainly an attractive technique for numerical analysis of the partial differential equations of motion. The problem areas of boundary conditions, need for smoothing (pseudo-viscosity?) lie with the theory and not with the solution technique. Future improvements would seem to depend largely upon developments in the theory since the numerical solution seems adequate.

Appendix B

CONVERGING-DIVERGING NOZZLE ANALYSIS COMPUTER PROGRAM

DISCUSSION

A computer program has been written to carry out the calculations discussed in the preceding sections of this report. This Appendix is written to explain the inner working of this program as well as its input-output.

GENERAL

The program is written in FORTRAN V language and with suitable alteration of dimension statements, can be utilized on machines with 16K (or greater) core locations. Input and output during execution is confined to the standard input and "listable" tapes. Conversion from machine to machine should therefore be readily accomplished. The program is an assembly of special or restricted purpose subroutines. These subroutines may be conveniently grouped as follows:

Subroutine Purpose	Subroutine Name
Driver	MAIN
Input	INPUT
Grid preparation	SETUP1
	SETUP2
	SETUP3
	SETUP4
	TRANSX
	TRANSR
	TRANSO
	WALL
Flowfield initialization	START
Error minimization control	LOGIC

Governing equation analyzers	EMT
	BOUND
Output	OUTPUT
Utility	ITSUB
	RHO

Before proceeding with an explanation of each subroutine it may be helpful to describe basically the organization of the computer program. The code was, as much as possible, written such that variable names were descriptive. This fact should help in the understanding of the program.

A main routine is written which acts as a driver for the entire subsequent calculation. Multiple or stacked cases are possible since the main program recycles to initiate the input routine. If all cases have been processed this attempt to read will terminate the job.

The sole function of the input routine is to get the necessary information into core and does essentially no processing. Assisting the input routine are four setup subroutines which are selected based on the input instructions and data required. Each of these routines upon completion of their function, returns to the input routine which in turn returns to the main program.

At that point all input requirements are satisfied and the physical grid and transformation derivatives have been determined. The next step is to make an initial flowfield estimate. For this estimate, subroutine START is called.

Upon completion of the initialization, the relaxation process is begun by entering subroutine LOGIC. This routine repetitively employs subroutines EMT and BOUND until a terminal condition is reached. Periodically the output subroutine is called. Upon termination of the calculation, control is returned to the main program which reinitiates the input.

SUBROUTINE DESCRIPTIONS

Subroutine: MAIN

This routine is an unchanging main program that seldom if ever needs recompiling.

Subroutine: INPUT

This subroutine is the basic input routine. The necessary input sequence is as follows:

Card 1, Format (20A4), header information, appears at the top of each page

Card 2, Format (16I5), options card, controls execution of program

Field 1, ΔΔΔΔX,	X =	number of boundary equations
Field 2, ΔΔXYZ,	X = 1,	automated setup (see SETUP1)
	X = 2,	input and distribution (see SETUP2)
	X = 3,	input all points (see SETUP3)
	X = 4,	input circular arcs (see SETUP4)
	Y = 0,	tube radial transformation (see TRANSR)
	Y = 1,	sine radial transformation (see TRANSR)
	Y 1	(see TRANSR)
	Z = 0	linear axial transformation (see TRANSX)
	Z = 1	tangent axial transformation (see TRANSX)
	Z 1	(see TRANSX)
Field 3, ΔΔΔXX,	XX =	number ψ cuts
Field 4, ΔΔΔXX,	XX =	number of ξ cuts
Field 5, ΔΔΔXX,	XX =	number of ξ cuts downstream of throat
Field 6, XXXXX,	XXXXX =	number of calculation steps/print step
Field 7, XXXXX,	XXXXX =	number of calculation steps to termination
Field 8, ΔΔΔΔX,	X =	number of ξ cuts/printed page
Field 9, ΔΔΔXY,	X = 0,	alter upstream boundary
	X = 1,	do not alter upstream boundary
	Y = 0,	alter downstream boundary
	Y = 1,	do not alter downstream boundary
Field 10, XXXXX,		number of calculation steps before smoothing employed.

Card 3, Format (5E10.6), gas reservoir conditions

Field 1-4, chamber pressure, temperature, gas constant, gamma

Card(s)* 4, Format (I1, 9X, 6E10.6), wall equations data

Field 1, X, X = 1 conic eq. $r = a\left\{\sqrt{b + cx + dx^2} + e\right\}$

X = 2 poly $r = ax^4 + bx^3 + cx^2 + dx + e$

X = 3 expon. $r = a(1 + e^{-bx^2}) + c$

Field 2-7 a, b, c, d, e, axial limit to which equation applies.

Card 5, Format (5E10.6), linear axial stretching factor, damping factor

Card(s)6, see subroutines SETUP1, SETUP2, SETUP3, SETUP4

Subroutine: SETUP1

This subroutine calculates the type of grid distribution shown in the sketch below. The actual distributions $r(\xi, \psi)$, $X(\xi, \psi)$ are determined by TRANSR, and TRANSX, respectively.

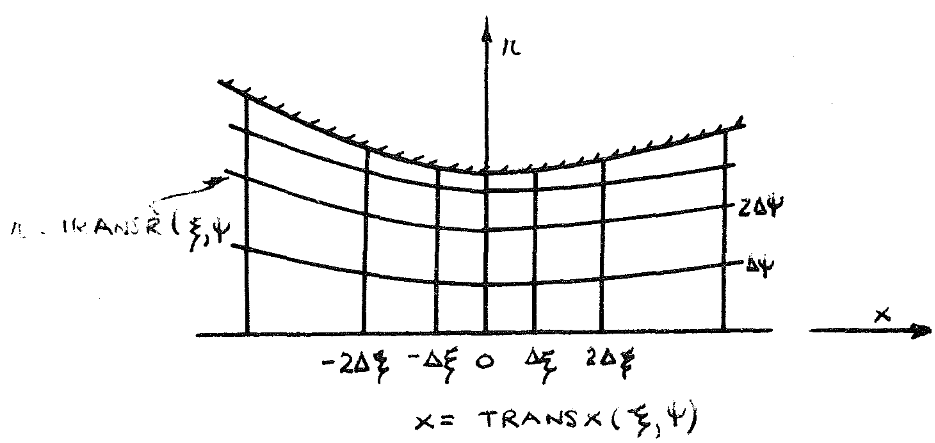

*Input as many cards as boundary equations beginning with equation farthest upstream

This type of grid distribution involves the least effort on the part of the user and should be satisfactory for many current rocket engines. Extremely high entrance angles should not be attempted with this distribution for obvious reasons.

An additional input parameter must be supplied to be read by this subroutine. This parameter is $\Delta\xi$ and for the tangent stretching transformation $\Delta\xi$ must be chosen such that the maximum value of $|\xi|$ is less than $\pi/2$.

Card 6, Format (E10.6), $\Delta\xi$

Subroutine: SETUP2

This subroutine gives much the same distribution as that above except that the user cannot find a convenient transformation X = TRANSX(ξ, ψ) and therefore wishes to input this transformation in a tabular form. Starting with the most upstream station input, list of axial locations for ξ data surfaces.

Cards 6, Format (8E10.6), (X(N), N=1, NTOT)

Subroutine: SETUP3

This subroutine reads the grid setup in its entirety. The wall equations need not be input with this option.

Cards 6, Format (8E10.6), (X(M, N), R(M, N), M=1, MTOT)

Subroutine: SETUP4

Referring to the sketch on the following page it can be seen that the grid distribution is determined along circular arcs. Generally these arcs are normal to the wall and center line. Occasionally this is not possible nor practical, particularly in the case of the axial inflow. It is for this reason that the wall angle is also input along with the basic information needed to determine the grid.

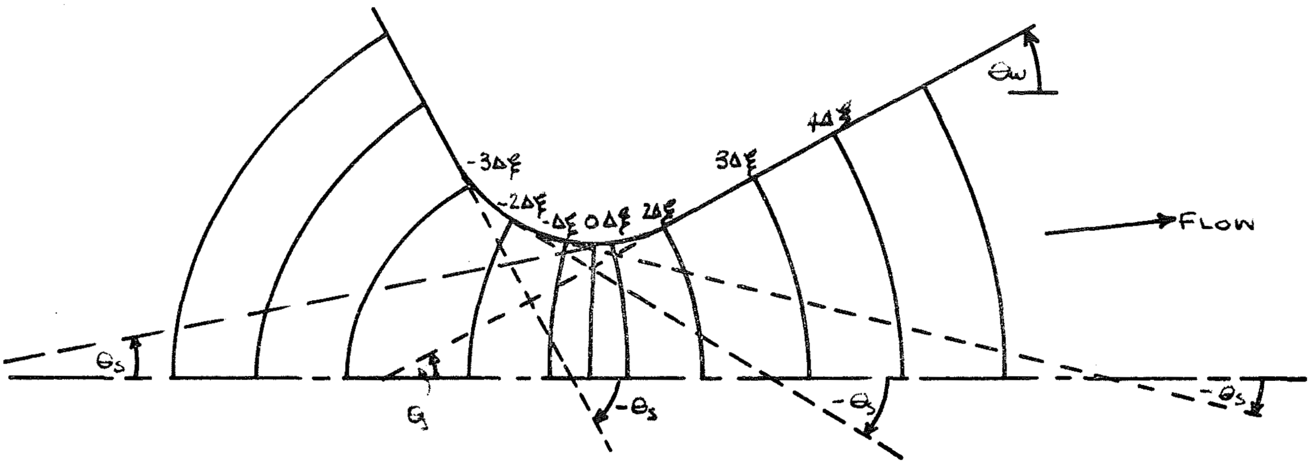

All ξ stations are input in order starting from the left. For all stations but the throat station a card containing the following information is supplied

Cards 6, Format (8E10.6), r_s, x_s, θ_s, θ_w

where x_s is the center of the circular arc, r_s is the radius of the arc, θ_s is the included angle (degrees) of the arc and θ_w is the wall angle (degrees) at arc wall intersection. The throat is a special case and requires a card with the throat radius in field one with the remaining fields blank.

It is not necessary to input the wall boundary conditions with this setup option.

Function TRANSX

This function provides one of two selectable transformations on call. They are

$$\left.\begin{aligned} x &= C\xi \\ x &= C\tan\left(\frac{\pi}{2}\xi\right) \end{aligned}\right\}$$ where C (axial stretching factor) was input (see Subroutines INPUT)

The function is designed such that other transformations may be easily added.

Function TRANSR

This function provides one of two selectable transformations on call. They are

$r = R_w(x)\ \psi$ where $R_w(x)$ is the wall radius determined from the boundary equations

$r = Rw(x)\ \sin\left(\frac{\pi}{2}\ \psi\right)$

This function is designed such that other transformations may easily be added.

Subroutine TRANSD

The purpose of this calculation is to provide the derivatives of the transformations that have been supplied. These derivatives are taken numerically.

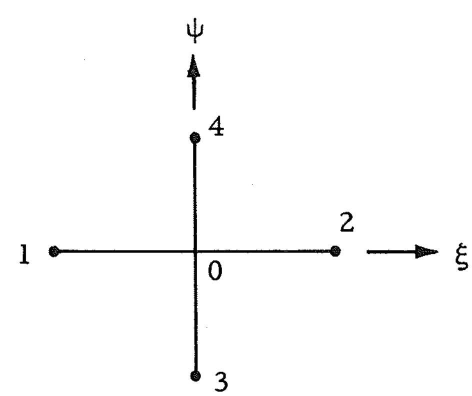

Using centered differences

$$r_\psi = \frac{r_4 - r_3}{2\Delta\psi} \quad ; \quad x_\psi = \frac{x_4 - x_3}{2\Delta\psi}$$

$$r\xi = \frac{r_2 - r_1}{2\Delta\xi} \; ; \; x\xi = \frac{x_2 - x_1}{2\Delta\xi}$$

The information which is actually retained for subsequent use is

$$2\Delta\psi\, r_\psi\,,\; 2\Delta\psi\, x_\psi,\; 2\Delta\zeta\, x_\zeta\,,\; 2\Delta\zeta\, x_\zeta$$

As it stands, this subroutine could be removed with an attendant savings in core since block common GRIDD contains information which can easily be recomputed as necessary.

Subroutine WALL

This subroutine calculates $R_w(x)$ using one of the three input equations described in Subroutine INPUT. Other functions could be included easily if desired.

Subroutine START

It is necessary to initialize the flow components to some reasonable values before beginning the relaxation process. The better the initial guess the faster one can expect an acceptable final solution. It is necessary to use some variation of one dimensional flow theory in order to make this initial approximation to the solution. With the grid distributions described in SETUP1, SETUP2, SETUP3 the constant ξ surface is initialized to have a constant Mach number, which if the flow were axial, would conserve the one-dimensional value of the choking mass flow.

With SETUP4, however, it is possible to make a better initial guess since the circular arcs (for $\theta_s = \theta_w$) correspond to constant Mach number surfaces for source or sink flow.

Subroutine LOGIC

The descent process described in Appendix A is implemented by this subroutine. This subroutine also prints a message each time the descent process is unsuccessful.

Subroutine EMT

This subroutine utilizes the equations derived in the main body of the report and the derivative equations found in Appendix A to calculate the error function and its derivatives for the entirety of the interior flow field points.

Subroutine BOUND

This subroutine utilizes the equations derived in the main body of the report and the derivatives equations found in Appendix A to calculate the derivative of the error function for the boundary points. If desired this subroutine can prevent either the inlet or the outlet or both surfaces from changing during the relaxation process. This is done by zeroing out the error function derivatives corresponding to these surfaces (see Field 9 of Card 2).

Subroutine OUTPUT

Periodically (determined by input) the OUTPUT subroutine is called. Its function is to output current values of flow variables over the entire flow field. The magnitude of the error function (6) as well as the descent step length (DELTA) are printed for this output relaxation step. The velocity components are given in ft/sec while the flow angle is given in degrees. The axial and radial position are output in the same units (any consistent units) which were input. The Mach number, and pressure and temperature ratios are, of course, dimensionless.

The mass flux through each surface and the wall thrust integral (initialized to zero at the leftmost station) are also calculated. The mass flow is divided by the one-dimensional value and is output as the mass flow coefficient. The thrust increment is divided by the chamber pressure and the throat area and is therefore also output as a dimensional quantity.

It is possible (see Subroutine INPUT) to control the number of ζ surfaces output per page so that an unnecessary amount of paper is not generated.

See Subroutine LOGIC for an additional print message.

Subroutine ITSUB

This general purpose routine is used to perform the iterative solution to a function of one variable, i.e., determine x such that $f(x) = 0$

Function RHO

This function calculates the density as a function of the velocity components.

Sample Input

The infinite reservoir, 0.25 radius of curvature, 90-deg inlet case discussed in the main body of the report is given below as a sample of the input required.

```
                                  JPL  90  DEG  INLET  ,.25  RC  ,  RESERVOIR  INFLOW
       1    400      11     19      8   400  2000      2     00  1600
+1         +04+1         +04+1768   +04+14        +01

+1         +01+3         -01
+25        +01-2         +00-9      +02-9         +02
+20        +01-2         +00-9      +02-9         +02
+15        +01-2         +00-9      +02-9         +02
+1         +01-2         +00-9      +02-9         +02
+98        +00+61        -01-75     +02-75        +02
+104       +01+346       +00-6      +02-6         +02
+121       +01+717       +00-45     +02-45        +02
+165       +01+1335      +01-30     +02-3         +02
+312       +01+296       +01-15     +02-15        +02
+615       +01+606       +01-75     +01-75        +01
+8         +00
+615       +01-606       +01+75     +01+75        +01
+312       +01-296       +01+15     +02+15        +02
+322       +01-296       +01+15     +02+15        +02
+342       +01-296       +01+15     +02+15        +02
+382       +01-296       +01+15     +02+15        +02
+452       +01-296       +01+15     +02+15        +02
+522       +01-296       +01+15     +02+15        +02
+602       +01-296       +01+15     +02+15        +02
```

JPL 75 DEG INLET ,.25 RC , RESERVØIR INFLØW

RELAXATIØN STEP 500 G= 0.1687E-04 DELTA= 0.1002E-01

R	X	U	V	M	THETA	P/PC	T/TC
0.8027E 00	-0.3739E-01	0.1724E 04	-0.2301E 03	0.1272E 01	-0.7602E 01	0.3748E 00	0.7555E 00
0.7928E 00	-0.3869E-01	0.1603E 04	-0.2778E 03	0.1166E 01	-0.9833E 01	0.4307E 00	0.7861E 00
0.7634E 00	-0.4244E-01	0.1482E 04	-0.2791E 03	0.1061E 01	-0.1066E 02	0.4911E 00	0.8161E 00
0.7152E 00	-0.4827E-01	0.1354E 04	-0.2907E 03	0.9574E 00	-0.1212E 02	0.5548E 00	0.8451E 00
0.6494E 00	-0.5562E-01	0.1256E 04	-0.2444E 03	0.8730E 00	-0.1101E 02	0.6086E 00	0.8677E 00
0.5676E 00	-0.6375E-01	0.1174E 04	-0.2178E 03	0.8067E 00	-0.1051E 02	0.6516E 00	0.8848E 00
0.4718E 00	-0.7188E-01	0.1118E 04	-0.1577E 03	0.7578E 00	-0.8029E 01	0.6835E 00	0.8970E 00
0.3644E 00	-0.7919E-01	0.1076E 04	-0.1264E 03	0.7238E 00	-0.6698E 01	0.7055E 00	0.9051E 00
0.2480E 00	-0.8500E-01	0.1053E 04	-0.7228E 02	0.7030E 00	-0.3928E 01	0.7190E 00	0.9100E 00
0.1256E 00	-0.8872E-01	0.1044E 04	-0.3817E 02	0.6952E 00	-0.2094E 01	0.7240E 00	0.9119E 00
-0.2114E-07	-0.9000E-01	0.1041E 04	0.4473E-05	0.6925E 00	0.2463E-06	0.7257E 00	0.9125E 00

MASS FLØW CØEFFICIENT= 0.9683E 00 THRUST INCREMENT= -0.7859E 01

```
C       MAIN
  100   CALL INPUT
        CALL START
        CALL LOGIC
        GO TO 100
        END
```

```
        SUBROUTINE SETUP1
        COMMON/OPTION/KOPT(16)
        COMMON/GRID/X(11,21),R(11,21)
   10   FORMAT(E10.6)
        MTOT=KOPT(3)
        NTOT=KOPT(4)
        ND=KOPT(5)
        READ(5,10)DXI
        XI=-FLOAT(NTOT-ND)*DXI
        DPSI=1./FLOAT(MTOT-1)
        DO 100 N=1,NTOT
        XI=XI+DXI
        PSI=1.+DPSI
        DO 100 M=1,MTOT
        PSI=PSI-DPSI
        X(M,N)=TRANSX(XI,PSI)
        R(M,N)=TRANSR(XI,PSI)
  100   CONTINUE
        RETURN
        END
```

```
      SUBROUTINE SETUP2
      COMMON/OPTION/KOPT(16)
      COMMON/GRID/X(11,21),R(11,21)
      DIMENSION XIN(21)
   10 FORMAT(8E10.5)
      MTOT=KOPT(3)
      NTOT=KOPT(4)
      READ(5,10)(XIN(N),N=1,NTOT)
      DPSI=1./FLOAT(MTOT-1)
      DO 100 N=1,NTOT
      XI=XIN(N)
      PSI=1.+DPSI
      DO 100 M=1,MTOT
      PSI=PSI-DPSI
      X(M,N)=TRANSX(XI,PSI)
      R(M,N)=TRANSR(XI,PSI)
  100 CONTINUE
      RETURN
      END
```

```
      SUBROUTINE SETUP3
      COMMON/OPTION/KOPT(16)
      COMMON/GRID/X(11,21),R(11,21)
   10 FORMAT(8E10.6)
      MTOT=KOPT(3)
      NTOT=KOPT(4)
      DO 100 N=1,NTOT
      READ(5,10)(X(M,N),R(M,N),M=1,MTOT)
  100 CONTINUE
      RETURN
      END
```

```
      SUBROUTINESETUP4
      COMMON/OPTION/KOPT(16)
      COMMON/GRID/X(11,21),R(11,21)
      COMMON/SOURCE/RS(21),XS(21),THETAS(21),THETWA(21)
      DATAPIO2/1.5707963/
   10 FORMAT(8E10.6)
      MTOT=KOPT(3)
      NTOT=KOPT(4)
      ND=KOPT(5)
      NS=NTOT-ND
      DPSI=1./FLOAT(MTOT-1)
      DO100N=1,NTOT
      READ(5,10)RS(N),XS(N),THETAS(N),THETWA(N)
      THETAS(N)=THETAS(N)/57.3
      THETWA(N)=THETWA(N)/57.3
      PSI=1.+DPSI
      DO100M=1,MTOT
      PSI=PSI-DPSI
      R(M,N)=RS(N)*SIN(ABS(THETAS(N)))*SIN(PIO2*PSI)
      IF(N.EQ.NS)R(M,N)=RS(N)*SIN(PIO2*PSI)
      F=1.
      IF(THETAS(N).LT.0.)F=-1.
      X(M,N)=XS(N)+F*SQRT(RS(N)**2-R(M,N)**2)
      IF(N.EQ.NS)X(M,N)=0.
  100 CONTINUE
      RETURN
      END
```

```
      FUNCTION TRANSX(XI,PSI)
      COMMON/OPTION/KOPT(16)
      COMMON/MISG/XSCALE,DAMP
      DATAPIO2/1.5707963/
      I=KOPT(2)-10 *(KOPT(2)/10 )
      IF(I.NE.0)GO TO 100
      TRANSX=XSCALE*XI
      GOTO1000
  100 IF(I.NE.1)GO TO 200
      TRANSX=XSCALE*SIN(PIO2*XI)/COS(PIO2*XI)
      GOTO1000
  200 CONTINUE
 1000 RETURN
      END
```

```
      FUNCTION TRANSR(XI,PSI)
      COMMON/OPTION/KOPT(16)
      DATAPI02/1.5707963/
      I=KOPT(2)/10-10*(KOPT(2)/100)
      IF(I.NE.0) GO TO 100
      X=TRANSX(XI,PSI)
      CALL WALL (RSCALE,X)
      TRANSR=RSCALE*PSI
      GO TO 1000
 100  IF(I.NE.1)GO TO 200
      X=TRANSX(XI,PSI)
      CALL WALL (RSCALE,X)
      TRANSR=RSCALE*SIN(PI02*PSI)
      GO TO 1000
  200 CONTINUE
 1000 RETURN
      END
```

```
      SUBROUTINE TRANSD
      COMMON/GRIDD/DXDXI(11,21),DXDPSI(11,21),DRDXI(11,21),DRDPSI(11,21)
      COMMON/GRID/X(11,21),R(11,21)
      COMMON/OPTION/KOPT(16)
      MTOT=KOPT(3)
      NTOT=KOPT(4)
      DO 1000 N=1,NTOT
      NM1=N-1
      NP1=N+1
      IF(N.EQ.1)NM1=N
      IF(N.EQ.NTOT)NP1=N
      DO 1000 M=1,MTOT
      MM1=M-1
      MP1=M+1
      IF(M.EQ.1)MM1=M
      IF(M.EQ.MTOT)MP1=M
      DXDXI(M,N)=Y(M,NP1)-X(M,NM1)
      DXDPSI(M,N)=X(MM1,N)-X(MP1,N)
      DRDXI(M,N)=R(M,NP1)-R(M,NM1)
      DRDPSI(M,N)=R(MM1,N)-R(MP1,N)
 1000 CONTINUE
      RETURN
      END
```

```
      SUBROUTINE WALL(R,X)
      COMMON/WALLFO/IWALL(10),WALLCO(10,6)
      COMMON/OPTION/KOPT(16)
      DIMENSION A(5)
      NBOUND=KOPT(1)
      DO 100 N=1,NBOUND
      IF(WALLCO(N,6).GT.X)GO TO 200
100   CONTINUE
      N=NBOUND
200   DO 300 J=1,5
300   A(J)=WALLCO(N,J)
      IW=IWALL(N)
      GO TO (400,500,600),IW
400   R=A(1)*(SQRT(A(2)+A(3)*X+A(4)*X*X)+A(5))
      GO TO 700
500   R=(((A(1)*X+A(2))*X+A(3))*X+A(4))*X+A(5)
      GO TO 700
600   E=EXP(-A(2)*X*X)
      R=A(1)*(1.-E)+A(3)
      GO TO 700
700   RETURN
      END
```

```
      FUNCTION RHO(U,V)
      COMMON/REST/PC,TC,RC,GAMMAC,RHOC,AC
      GM1=GAMMAC-1.
      RHO=(1.-.5*GM1*(U*U+V*V))**(1./GM1)
      RETURN
      END
```

```
      SUBROUTINE ITSUB (FOFY,Y,SAVE,CONV,NTIMES)
C     SUBROUTINE FOR REGULI FALSI ITERATION CONTROL
C
C
      DIMENSIONSAVE(8)
      N1=SAVE(3) +.1
      FOFXCK=SAVE(8)
      FOFX=FOFY
      X=Y
      IF(ABS (FOFX)-CONV.LE.0.)GOTO110
      ITIME=SAVE(1)+.1
      GOTO(10,30,50,70),ITIME
   10 N1=1
      ITIME=2
      FOFXCK=FOFX
      SAVE(8)=FOFXCK
      IF(FOFX.LT.0.)GOTO50
   30 IF(FOFX.LT.0.)GOTO70
      IF(FOFXCK.GE.FOFX)GOTO35
      SAVE(2)=-1.*SAVE(2)
      X=X-2.*SAVE(2)
      GOTO90
   35 SAVE(4)=X
      SAVE(5)=FOFX
      X=X-SAVE(2)
      GOTO90
   50 ITIME=3
      IF(FOFX.GT.0.)GOTO70
      IF(FOFXCK.LE.FOFX)GOTO55
      SAVE(2)=-1.*SAVE(2)
      X=X+2.*SAVE(2)
      GOTO90
   55 SAVE(6)=X
      SAVE(7)=FOFX
      X=X+SAVE(2)
      GOTO90
   70 ITIME=4
      N1=SAVE(3)
```

```
      IF(FOFX.LT.0.)GOTO75
      SAVE(4)=X
      SAVE(5)=FOFX
      GOTO80
   75 SAVE(6)=X
      SAVE(7)=FOFX
   80 X=SAVE(4)-SAVE(5)*((SAVE(6)-SAVE(4))/(SAVE(7)-SAVE(5)))
   90 IF(N1.GE.NTIMES)GOTO100
      N1=N1+1
      SAVE(3)=N1
      GOTO120
  100 ITIME=6
      GOTO120
  110 ITIME=5
      SAVE(4)=X
      SAVE(5)=FOFX
      SAVE(6)=X
      SAVE(7)=FOFX
  120 SAVE(1)=FLOAT(ITIME)+.1
      Y=X
      RETURN
      END
```

```
      SUBROUTINE OUTPUT(L)
      COMMON/OPTION /KOPT(16)
      COMMON/GRID/X(11,21),R(11,21)
      COMMON/FLOW/U(11,21),V(11,21)
      COMMON/REST/PC,TC,RC,GAMMAC,RHOC,AC
      COMMON/HEADER/HEAD(20)
      COMMON/MISCD/G,GM1,DEL
      COMMON/GRIDD/DXDXI(11,21),DXDPSI(11,21),DRDXI(11,21),DRDPSI(11,21)
      DATAPI/3.14159/
   10 FORMAT(1H1,20A4)
   20 FORMAT(17HORELAXATION STEP ,I5,3H G=,E12.4,7H DELTA=,E12.4)
   30 FORMAT(1H0,11X,1HR,11X,1HX,11X,1HU,11X,1HV,11X,1HM,7X,5HTHETA
     1,8X,4HP/PC,8X,4HT/TC)
   40 FORMAT(1H0,8E12.4)
   50 FORMAT(1H0,22HMASS FLOW COEFFICIENT=,E12.4,18H THRUST INCREMENT=,
     1E12.4)
      MTOT=KOPT(3)
      NTOT=KOPT(4)
      NPAGE=KOPT(8)
      NS=NTOT-KOPT(5)
      AS=PI*R(1,NS)*R(1,NS)
      US=SQRT(2./(GAMMAC+1.))
      RHOS=RHO(US,0.)
      WONED=RHOS*US*AS
      GOGM1=GAMMAC/(GAMMAC-1.)
      PINTEG=0.
      DO 2000 N=1,NTOT
      IF(N-NPAGE*(N/NPAGE).EQ.1)WRITE(6,10)HEAD
      WRITE(6,20)L,G,DEL
      WRITE(6,30)
      W=0.
      IF(N.EQ.1)GOTO500
      P2=(1.-(GAMMAC-1.)*.5*(U(1,N)**2+V(1,N)**2))**GOGM1
      P1=(1.-(GAMMAC-1.)*.5*(U(1,N-1)**2+V(1,N-1)**2)) **GOGM1
      PINTEG=PINTEG+(P2+P1)*.5*PI*(R(1,N)**2-R(1,N-1)**2)/AS
  500 DO 1000 M=1,MTOT
      UP=U(M,N)*AC
      VP=V(M,N)*AC
```

```
      QSQ=UP*UP+VP*VP
      T=TC-(GAMMAC-1.)*.5*QSQ/(GAMMAC*RC)
      EMP=SQRT(QSQ/(GAMMAC*RC*T))
      THETA=57.3*ATAN(VP/UP)
      TOTC=T/TC
      POPC=(TOTC)**(GAMMAC/(GAMMAC-1.))
      WRITE(6,40)R(M,N),X(M,N),UP,VP,EMP,THETA,POPC,TOTC
      RHOP=POPC/TOTC
      MM1=M-1
      MP1=M+1
      IF(M.EQ.1)MM1=M
      IF(M.EQ.MTOT)MP1=MTOT
      DA=PI*(R(MM1,N)+R(MP1,N))*.5
      W=W+DA*RHOP*(U(M,N)*DRDPSI(M,N)-V(M,N)*DXDPSI(M,N))
 1000 CONTINUE
      WRAT=W/WONED
      WRITE(6,50)WRAT,PINTEG
 2000 CONTINUE
      RETURN
      END
```

```
      SUBROUTINE INPUT
      COMMON/HEADER/HEAD(20)
      COMMON/OPTION/KOPT(16)
      COMMON/REST/PC,TC,RC,GAMMAC,RHOC,AC
      COMMON/WALLFO/IWALL(10),WALLCO(10,6)
      COMMON/MISCG/XSCALE,DAMP
   10 FORMAT(20A4)
   20 FORMAT(16I5)
   30 FORMAT(5E10.6)
   40 FORMAT(I1,9X,6E10.6)
   50 FORMAT(1H1,20A4)
   60 FORMAT(5H OPT(,I2,2H)=,I5)
   70 FORMAT(4H PC=,E12.4,3HTC=,E12.4,3HRC=,E12.4,7HGAMMAC=,E12.4)
   80 FORMAT(6H0IWALL,11X,1HA,11X,1HB,11X,1HC,11X,1HD,11X,1HE,9X,3HMAX)
   90 FORMAT(1H ,4X,I1,6E12.4)
      READ(5,10)HEAD
      WRITE(6,50)HEAD
      READ(5,20)KOPT
      DO 100 I=1,10
      WRITE(6,60)I,KOPT(I)
  100 CONTINUE
      READ(5,30)PC,TC,RC,GAMMAC
      WRITE(6,70)PC,TC,RC,GAMMAC
      RHOC=PC/(RC*TC)
      AC=SQRT(GAMMAC*RC*TC)
      IB=KOPT(1)
      IF(IB.EQ.0)GOTO200
      READ(5,40)(IWALL(I),(WALLCO(I,J),J=1,6),I=1,IB)
      WRITE(6,80)
      WRITE(6,90)(IWALL(I),(WALLCO(I,J),J=1,6),I=1,IB)
  200 READ(5,30)XSCALE,DAMP
      I=KOPT(2)/100
      IF(I.EQ.1)CALL SETUP1
      IF(I.EQ.2)CALL SETUP2
      IF(I.EQ.3)CALL SETUP3
      IF(I.EQ.4)CALLSETUP4
      CALL TRANSD
      RETURN


       END
```

```
      SUBROUTINE START
      COMMON/GRID/X(11,21),R(11,21)
      COMMON/FLOW/U(11,21),V(11,21)
      COMMON/REST/PC,TC,RC,GAMMAC,RHOC,AC
      COMMON/OPTION/KOPT(16)
      COMMON/GRIDD/DXDXI(11,21),DXDPSI(11,21),DRDXI(11,21),DRDPSI(11,21)
      COMMON/ENDC/ULEND(11),VLEND(11),UREND(11),VREND(11)
      COMMON/SOURCE/RSS(21),XSS(21),THETAS(21),THETWA(21)
      DIMENSION SAVE(8)
      DATAPI/3.14159/
      MTOT=KOPT(3)
      NTOT=KOPT(4)
      ND=KOPT(5)
      NS=NTOT-ND
      US=SQRT(2./(GAMMAC+1.))
      RHOS=RHO(US,0.)
      WONED=PI*RHOS*US*R(1,NS)*R(1,NS)
      U(1,NS)=US
      NSM1=NS-1
      IF(KOPT(2)/100.EQ.4)GOTO6000
      IF(NSM1.EQ.0)GOTO1050
      UW=US*.9
      DO 1000 I=1,NSM1
      SAVE(1)=1.
      SAVE(2)=.0049*UW
      N=NS-I
      RW=R(1,N)
      A=PI*RW*RW
100   CALL ITSUB(RHO(UW,0.)*UW*A-WONED,UW,SAVE,.001*WONED,99)
      IF(UW.GT.US)UW=US
      IBR=SAVE(1)
      GOTO (100,100,100,100,200,200),IBR
 200  U(1,N)=UW
1000  CONTINUE
1050  UW=US*1.1
      DO 2000 I=1,ND
      SAVE(1)=1.
      SAVE(2)=.049*US
```

```
      N=NS+1
      RW=R(1,N)
      A=PI*RW*RW
 1100 CALL ITSUB(RHO(UW,0.)*UW*A-WONED,UW,SAVE,.001*WONED,99)
      IF(UW.LT.US)UW=US
      IBR=SAVE(1)
      GO TO (1100,1100,1100,1100,1200,1200),IBR
 1200 U(1,N)=UW
 2000 CONTINUE
      DO 3000 N=1,NTOT
      Q=U(1,N)
      DO 3000 M=1,MTOT
      DS=SQRT(DXDXI(M,N)**2+DRDXI(M,N)**2)
      U(M,N)=Q*DXDXI(M,N)/DS
      V(M,N)=Q*DRDXI(M,N)/DS
 3000 CONTINUE
      N=NTOT
      TANTW=DRDXI(1,N)/DXDXI(1,N)
      THETAW=ATAN(TANTW)
      IF(THETAW.LT..05)GOTO4000
      RW=R(1,N)
      XS=-RW/TANTW
      DO3500M=1,MTOT
      RP=R(M,N)
      RS=SQRT(XS*XS+RP*RP)
      THETA=ATAN(RP*TANTW/RW)
      A=2.*PI*RS*RS*(1.-COS(THETAW))/COS(THETA)
      TANTP=SIN(THETA)/COS(THETA)
      SAVE(1)=1.
      SAVE(2)=.05*UW
 3100 VW=UW*TANTP
      CALLITSUB(RHO(UW,VW)*UW*A-WONED,UW,SAVE,.001*WONED,99)
      IBR=SAVE(1)
      GOTO(3100,3100,3100,3100,3200,3200),IBR
 3200 U(M,N)=UW
      V(M,N)=VW
 3500 CONTINUE
 4000 CONTINUE
```

```
      DO5000M=1,MTOT
      ULEND(M)=U(M,1)
      VLEND(M)=V(M,1)
      UREND(M)=U(M,NTOT)
      VREND(M)=V(M,NTOT)
 5000 CONTINUE
      GOTO7000
 6000 DO6100M=1,MTOT
      U(M,NS)=US
 6100 V(M,NS)=0.
      Q=.9*US
      DO6200I=1,NSM1
      IF(Q.GT..9*US)Q=.9*US
      N=NS-I
      A=2.*PI*RSS(N)*RSS(N)*(1.-COS(THETAS(N)))
      SAVE(1)=1.
      SAVE(2)=.05*US
 6050 CALLITSUB(RHO(Q,0.)*Q*A-WONED,Q,SAVE,.001*WONED,99)
      IF(Q.GT.US)Q=US
      IBR=SAVE(1)
      GOTO(6050,6050,6050,6050,6150,6150),IBR
 6150 DO6200M=1,MTOT
      TANT=R(M,N)/(X(M,N)-XSS(N))
      THET=ATAN(TANT)*THETWA(N)/THETAS(N)
      U(M,N)=Q*COS(THET)
      V(M,N)=Q*SIN(THET)
 6200 CONTINUE
      Q=1.1*US
      DO6400I=1,ND
      IF(Q.LT.1.1*US)Q=1.1*US
      N=NS+I
      A=2.*PI*RSS(N)*RSS(N)*(1.-COS(THETAS(N)))
      SAVE(1)=1.
      SAVE(2)=.05*US
 6250 CALLITSUB(RHO(Q,0.)*Q*A-WONED,Q,SAVE,.001*WONED,99)
      IF(Q.LT.US)Q=US
      IBR=SAVE(1)
      GOTO(6250,6250,6250,6250,6300,6300),IBR


 6300 DO6400M=1,MTOT
      TANT=R(M,N)/(X(M,N)-XSS(N))
      THET=ATAN(TANT)*THETWA(N)/THETAS(N)
      U(M,N)=Q*COS(THET)
      V(M,N)=Q*SIN(THET)
 6400 CONTINUE
 7000 CONTINUE
      RETURN
      END
```

```
      SUBROUTINE BOUND
      COMMON/FLOW/U(11,21),V(11,21)
      COMMON/DECENT/DGDU(11,21),DGDV(11,21)
      COMMON/GRIDD/DXDXI(11,21),DXDPSI(11,21),DRDXI(11,21),DRDPSI(11,21)
      COMMON/OPTION/KOPT(16)
      COMMON/MISCD/G,GM1,DEL
      COMMON/ENDC/ULEND(11),VLEND(11),UREND(11),VREND(11)
      COMMON/GRID/X(11,21),R(11,21)
      MTOT=KOPT(3)
      NTOT=KOPT(4)
      NTOTM1=NTOT-1
      DO300N=2,NTOTM1
      DX=DXDXI(1,N)
      DR=DRDXI(1,N)
      RHS=2.*(U(2,N)*DGDU(2,N)+V(2,N)*DGDV(2,N))-(U(3,N)*DGDU(3,N)+V(3,N)
     1)*DGDV(3,N))
      IF(ABS(DX).GT.ABS(DR))GOTO100
      DGDV(1,N)=RHS/(V(1,N)*(1.+DX*DX/(DR*DR)))
      DGDU(1,N)=DGDV(1,N)*DX/DR
      GOTO200
  100 DGDU(1,N)=RHS/(U(1,N)*(1.+DR*DR/(DX*DX)))
      DGDV(1,N)=DGDU(1,N)*DR/DX
  200 DGDU(MTOT,N)=(4.*DGDU(MTOT-1,N)-DGDU(MTOT-2,N))/3.
      DGDV(MTOT,N)=0.
  300 CONTINUE
      IF(KOPT(9)/10.EQ.0)GOTO500
      DO400M=1,MTOT
      DGDU(M,1)=0.
  400 DGDV(M,1)=0.
  500 IF(KOPT(9)-10*(KOPT(9)/10).EQ.0)GOTO700
      DO600M=1,MTOT
      DGDU(M,NTOT)=0.
  600 DGDV(M,NTOT)=0.
  700 CONTINUE
      RETURN
      END
```

```
      SUBROUTINE LOGIC
      COMMON/DECENT/DGDU(11,21),DGDV(11,21)
      COMMON/LASTEP/DGDU1(11,21),DGDV1(11,21)
      COMMON/FLOW/U(11,21),V(11,21)
      COMMON/OPTION/KOPT(16)
      COMMON/MISCD/G,GM1,DEL
      COMMON/MISG/XSCALE,DAMP
      COMMON/SMOOTH/SMULT
   10 FORMAT(1H ,3E12.4)
      L=-1
      MTOT=KOPT(3)
      NTOT=KOPT(4)
      NTOTM1=NTOT-1
      MTOTM1=MTOT-1
      SMULT=0.
      ISM=KOPT(10)
      GM1=1.E+16
      DEL=1.
  100 GRAD=0.
      G=0.
      DO 200 N=1,NTOT
      DO 200 M=1,MTOT
      DGDU(M,N)=0.
  200 DGDV(M,N)=0.
      CALL EMT
      CALL BOUND
      IF(G.GE.GM1)GO TO 1000
      GM1=G
      L=L+1
      DO 300 N=1,NTOT
      DO 300 M=1,MTOT
  300 GRAD=GRAD+DGDU(M,N)*DGDU(M,N)+DGDV(M,N)*DGDV(M,N)
      IF(L.EQ.KOPT(6)*(L/KOPT(6)))CALL OUTPUT(L)
      IF(L.EQ.ISM)GOTO600
      IF(L.GE.KOPT(7))GOTO2000
  400 SCALE=G/GRAD
  450 CONTINUE
      DO 500 N=1,NTOT
```

```
      DO 500 M=1,MTOT
      DGDU1(M,N)=DGDU(M,N)
      DGDV1(M,N)=DGDV(M,N)
      U(M,N)=U(M,N)-SCALE*DEL*DGDU(M,N)
      V(M,N)=V(M,N)-SCALE*DEL*DGDV(M,N)
  500 CONTINUE
      GO TO 100
  600 SMULT=DAMP
      GM1=1.E+16
      GOTO100
 1000 IF(DEL.LT..1E-8)GOTO1500
      WRITE(6,10)G,GM1,DEL
      DO 1100 N=1,NTOT
      DO 1100 M=1,MTOT
      DGDU(M,N)=DGDU1(M,N)
      DGDV(M,N)=DGDV1(M,N)
      U(M,N)=U(M,N)+SCALE*DEL*DGDU(M,N)
 1100 V(M,N)=V(M,N)+SCALE*DEL*DGDV(M,N)
      DEL=.75*DEL
      G=GM1
      GOTO450
 1500 CALLOUTPUT(L)
 2000 RETURN
      END
```

```
SUBROUTINE EMT
COMMON/GRIDD/DXDXI(11,21),DXDPSI(11,21),DRDXI(11,21),DRDPSI(11,21)
COMMON/DECENT/DGDU(11,21),DGDV(11,21)
COMMON/FLOW/U(11,21),V(11,21)
COMMON/MISCD/G,GM1,DEL
COMMON/OPTION/KOPT(16)
COMMON/REST/PC,TC,RC,GAMMAC,RHOC,AC
COMMON/GRID/X(11,21),R(11,21)
COMMON/SMOOTH/SMULT
MTOT=KOPT(3)
NTOT=KOPT(4)
MTOTM1=MTOT-1
NTOTM1=NTOT-1
NS=NTOT-KOPT(5)
GAMM1=GAMMAC-1.
DO 1000 N=2,NTOTM1
FNEXP=ABS(FLOAT(N-NS))
FNEXP=SQRT(FNEXP)
S=1./EXP(FNEXP)
DO 1000 M=2,MTOTM1
NM1=N-1
NP1=N+1
MM1=M-1
MP1=M+1
U0=U(M,N)
V0=V(M,N)
RHO0=RHO(U0,V0)
U1=U(M,NM1)
V1=V(M,NM1)
U2=U(M,NP1)
V2=V(M,NP1)
U4=U(MM1,N)
V4=V(MM1,N)
U3=U(MP1,N)
V3=V(MP1,N)
RPSI=R(MM1,N)-R(MP1,N)
RXI=R(M,NP1)-R(M,NM1)
XPSI=X(MM1,N)-X(MP1,N)
```

```
      XXI=X(M,NP1)-X(M,NM1)
      ALPHA=RPSI*XXI-RXI*XPSI
      RO=R(M,N)
      SA=6.2832*RO*SQRT(RPSI*RPSI+XPSI*XPSI)
      SA=SA/(R(1,N)*R(1,N))
      TRHO=1./RHOO**GAMM1
      ORHOSQ=1./(TRHO*TRHO)
      T1=RPSI*(U2-U1)-XPSI*(V2-V1)+XXI*(V4-V3)-RXI*(U4-U3)+ALPHA*V0/RO
      T2=RPSI*U0-XPSI*V0
      T3=U0*(U2-U1)+V0*(V2-V1)
      T4=XXI*V0-RXI*U0
      T5=U0*(U4-U3)+V0*(V4-V3)
      T6=T2*T3+T4*T5
      E1MN=T1-TRHO*T6
      E2MN=RPSI*(V2-V1)-RXI*(V4-V3)+XPSI*(U2-U1)-XXI*(U4-U3)
      E1MN=E1MN*S
      E2MN=E2MN*S
      E1MN=E1MN*SA
      G=G+.5*(E1MN*E1MN+E2MN*E2MN)
      E1MN=E1MN*SA
      E1MN=E1MN*S
      E2MN=E2MN*S
      SM=S*SMULT
      E3MN=U2+U1-2.*U0
      E4MN=V2+V1-2.*V0
      E5MN=U4+U3-2.*U0
      E6MN=V4+V3-2.*V0
      E3MN=E3MN*SM
      E4MN=E4MN*SM
      E5MN=E5MN*SM
      E6MN=E6MN*SM
      G=G+.5*(E3MN*E3MN+E4MN*E4MN+E5MN*E5MN+E6MN*E6MN)
      E3MN=E3MN*SM
      E4MN=E4MN*SM
      E5MN=E5MN*SM
      E6MN=E6MN*SM
      DGDU(M,N)=DGDU(M,N)-E1MN*(GAMM1*U0*T6*ORHOSQ
     1+TRHO*(RPSI*T3+T2*(U2-U1)-RXI*T5+T4*(U4-U3)))
```

```
     2-E3MN*2.-E5MN*2.
      DGDV(M,N)=DGDV(M,N)-E1MN*(-ALPHA/RO+GAMM1*VO*T6*ORHOSQ
     1+TRHO*(-XPSI*T3+T2*(V2-V1)+XXI*T5+T4*(V4-V3)))
     2-E4MN*2.-E6MN*2.
      DU2=E1MN*(RPSI-TRHO*T2*U0)+E2MN*XPSI
      DV2=E1MN*(-XPSI-TRHO*T2*V0)+E2MN*RPSI
      DU4=E1MN*(-RXI-TRHO*T4*U0)-E2MN*XXI
      DV4=E1MN*(XXI-TRHO*T4*V0)-E2MN*RXI
      DGDU(M,NP1)=DGDU(M,NP1)+DU2
     1+E3MN
      DGDV(M,NP1)=DGDV(M,NP1)+DV2
     1+E4MN
      DGDU(M,NM1)=DGDU(M,NM1)-DU2
     1+E3MN
      DGDV(M,NM1)=DGDV(M,NM1)-DV2
     1+E4MN
      DGDU(MM1,N)=DGDU(MM1,N)+DU4
     1+E5MN
      DGDV(MM1,N)=DGDV(MM1,N)+DV4
     1+E6MN
      DGDU(MP1,N)=DGDU(MP1,N)-DU4
     1+E5MN
      DGDV(MP1,N)=DGDV(MP1,N)-DV4
     1+E6MN
1000  CONTINUE
      RETURN
      END
```

Appendix C

DISTRIBUTION LIST FOR CONTRACT NAS7-743

DISTRIBUTION LIST FOR FINAL REPORT

CONTRACT NAS7-743

COPIES	RECIPIENT	DESIGNEE
	NASA HEADQUARTERS WASHINGTON, D.C. 20546	
1	CONTRACTING OFFICER	(X)
1	PATENT OFFICE	(X)
	NASA LEWIS RESEARCH CENTER 21000 BROOKPARK RD. CLEVELAND, OHIO 44135	
1	OFFICE OF TECHNICAL INFORMATION	(X)
1	CONTRACTING OFFICER	(X)
	NASA MANNED SPACECRAFT CENTER HOUSTON, TEXAS 77001	
1	OFFICE OF TECHNICAL INFORMATION	(X)
1	CONTRACTING OFFICER	(X)
1	PATENT OFFICE	(X)
	NASA MARSHALL SPACE FLIGHT CENTER HUNTSVILLE, ALABAMA 35812	
2	OFFICE OF TECHNICAL INFORMATION, MS-IP	(X)
1	PURCHASING OFFICE, PR-EC	(X)
1	PATENT OFFICE, M-PAT	(X)
1	TECHNOLOGY UTILIZATION OFFICE, MS-T	(X)
	NASA PASADENA OFFICE 4800 OAK GROVE DRIVE PASADENA, CALIFORNIA 91103	
1	PATENTS AND CONTRACTS MANAGEMENT	(X)
3	CONTRACTING OFFICER, F. ABBOTT	(X)
	JET PROPULSION LABORATORY 4800 OAK GROVE DR. PASADENA , CALIF. 91103	
20	R. F. CUFFEL	(X)
3	CHIEF, LIQUID EXPERIMENTAL ENGINEERING, RPL OFFICE OF ADVANCED RESEARCH AND TECHNOLOGY	(X)

NASA HEADQUARTERS
WASHINGTON, D.C., 20546

1 DIRECTOR, TECHNOLOGY UTILIZATION DIVISION (X)
OFFICE OF TECHNOLOGY UTILIZATION
NASA HEADQUARTERS
WASHINGTON, D.C. 20546

20 NASA SCIENTIFIC AND TECHNICAL INFORMATION FACILITY (X)
P.O. BOX 33
COLLEGE PARK, MARYLAND 20740

1 DIRECTOR , LAUNCH VEHICLES AND PROPULSION , SV (X)
OFFICE OF SPACE SCIENCE AND APPLICATIONS
NASA HEADQUARTERS
WASHINGTON , D. C. 20546

1 DIRECTOR, ADVANCED MANNED MISSIONS, MT (X)
OFFICE OF MANNED SPACE FLIGHT
NASA HEADQUARTERS
WASHINGTON , D. C. 20546

1 MISSION ANALYSIS DIVISION (X)
NASA AMES RESEARCH CENTER
MOFFETT FIELD, CALIFORNIA 24035

NASA FIELD CENTERS

2	AMES RESEARCH CENTER MOFFETT FIELD, CALIFORNIA 94035	HANS M. MARK
1	GODDARD SPACE FLIGHT CENTER GREENBELT, MARYLAND 20771	MERLAND L. MOSESON CODE 620
2	JET PROPULSION LABORATORY CALIFORNIA INSTITUTE OF TECHNOLOGY 4800 OAK GROVE DRIVE PASADENA, CALIFORNIA 91103	HENRY BURLAGE, JR PROPULSION DIV. 38
2	LANGLEY RESEARCH CENTER LANGLEY STATION HAMPTON, VIRGINIA 23365	ED CORTWRIGHT DIRECTOR
2	LEWIS RESEARCH CENTER 21000 BROOKPARK ROAD CLEVELAND, OHIO 44135	DR. ABE SILVERSTEIN DIRECTOR
2	MARSHALL SPACE FLIGHT CENTER HUNTSVILLE, ALABAMA 35812	HANS G. PAUL CODE R-P+VED
2	MANNED SPACECRAFT CENTER HOUSTON, TEXAS 77001	J.G. THIBODAUX, JR. CHIEF, PROP. + POWER DIV.
2	JOHN F. KENNEDY SPACE CENTER, NASA COCOA BEACH, FLORIDA 32931	DR. KURT H. DEBUS

GOVERNMENT INSTALLATIONS

1	AERONAUTICAL SYSTEMS DIVISION AIR FORCE SYSTEMS COMMAND WRIGHT-PATTERSON AIR FORCE BASE DAYTON, OHIO 45433	D.L. SCHMIDT CODE ASRCNC-2
1	AIR FORCE MISSILE DEVELOPMENT CENTER HOLLOMAN AIR FORCE BASE NEW MEXICO 88330	MAJ. R.E. BRACKEN
1	AIR FORCE MISSILE TEST CENTER PATRICK AIR FORCE BASE, FLORIDA	L.J. ULLIAN
1	SPACE AND MISSILE SYSTEMS ORGANIZATION AIR FORCE UNIT POST OFFICE LOS ANGELES 45, CALIFORNIA 90045	COL. CLARK TECHNICAL DATA CENTER
1	ARNOLD ENGINEERING DEVELOPMENT CENTER ARNOLD AIR FORCE STATION TULLAHOMA, TENNESSEE 37388	DR. H.K. DOETSCH
1	BUREAU OF NAVAL WEAPONS DEPARTMENT OF THE NAVY WASHINGTON , D. C. 20546	J. KAY RTMS-41
1	DEFENSE DOCUMENTATION CENTER HEADQUARTERS CAMERON STATION, BUILDING 5 5010 DUKE STREET ALEXANDRIA, VIRGINIA 22314 ATTN- TISIA	
1	HEADQUARTERS, U.S. AIR FORCE WASHINGTON 25, D.C. 20546	COL.C.K. STAMBAUGH AFRST
1	PICATINNY ARSENAL DOVER, NEW JERSEY 07801	I. FORSTEN, CHIEF LIQUID PROPULSION LABORATORY,
2	AIR FORCE ROCKET PROPULSION LABORATORY RESEARCH AND TECHNOLOGY DIVISION AIR FORCE SYSTEMS COMMAND EDWARDS, CALIFORNIA 93523	RPRPD/MR. H. MAIN
1	U.S. ARMY MISSILE COMMAND REDSTONE ARSENAL ALABAMA 35809	MR. WALTER WHARTON
1	U.S. NAVAL ORDNANCE TEST STATION CHINA LAKE CALIFORNIA 93557	CODE 4562 CHIEF, MISSILE PROPULSION DIV.

CPIA

1	CHEMICAL PROPULSION INFORMATION AGENCY APPLIED PHYSICS LABORATORY 8621 GEORGIA AVENUE SILVER SPRING, MARYLAND 20910	TOM REEDY

INDUSTRY CONTRACTORS

1	AEROJET-GENERAL CORPORATION P. O. BOX 1947 TECHNICAL LIBRARY, BLDG 2015, DEPT. 2410 SACRAMENTO, CALIFORNIA 95809	R. STIFF
1	AEROSPACE CORPORATION 2400 EAST EL SEGUNDO BOULEVARD P. O. BOX 95085 LOS ANGELES, CALIFORNIA 90045	JOHN G. WILDER MS-2293
1	ATLANTIC RESEARCH CORPORATION EDSALL ROAD AND SHIRLEY HIGHWAY ALEXANDRIA, VIRGINIA 22314	DR. RAY FRIEDMAN
1	BELL AEROSPACE COMPANY P.O. BOX 1 BUFFALO, NEW YORK 14240	W. M. SMITH
1	BELLCOMM 955 L-ENFANT PLAZA, S. W. WASHINGTON, D. C.	H. S. LONDON
1	BOEING COMPANY P. O. BOX 3707 SEATTLE, WASHINGTON 98124	J. D. ALEXANDER
1	WRIGHT AERONAUTICAL DIVISION CURTISS-WRIGHT CORPORATION WOOD-RIDGE, NEW JERSEY 07075	G. KELLEY
1	REPUBLIC AVIATION CORPORATION FAIRCHILD HILLER CORPORATION FARMINGDALE, LONG ISLAND, NEW YORK	LIBRARY
1	GENERAL DYNAMICS, CONVAIR DIVISION LIBRARY + INFORMATION SERVICES (128-00) P. O. BOX 1128	FRANK DORE
1	MISSILE AND SPACE SYSTEMS CENTER GENERAL ELECTRIC COMPANY VALLEY FORGE SPACE TECHNOLOGY CENTER P.O. BOX 8555 PHILADELPHIA, PA.	F. MEZGER F. E. SCHULTZ
1	GRUMMAN AIRCRAFT ENGINEERING CORP. BETHPAGE, LONG ISLAND	JOSEPH GAVIN

	NEW YORK 11714	
1	HONEYWELL, INC. AEROSPACE DIV. 2600 RIDGWAY RD MINNEAPOLIS, MINN.	MR. GORDON HARMS
1	HUGHES AIRCRAFT CO. AEROSPACE GROUP CENTINELA AND TEALE STREETS CULVER CITY, CALIF. 90230	E. H. MEIER V.P. AND DIV. MGR., RESEARCH + DEV. DIV.
1	WALTER KIDDE AND COMPANY, INC. AEROSPACE OPERATIONS 567 MAIN STREET BELLEVILLE, NEW JERSEY	R. J. HANVILLE DIR. OF RESEARCH ENGR.
1	LOCKHEED MISSILES AND SPACE CO. ATTN-TECHNICAL INFORMATION CENTER P.O. BOX 504 SUNNYVALE, CALIFORNIA 94088	J. GUILL
1	LOCKHEED PROPULSION COMPANY P. O. BOX 111 REDLANDS, CALIFORNIA 92374	H. L. THACKWELL
1	THE MARQUARDT CORPORATION 16555 SATICOY STREET VAN NUYS ,CALIF. 91409	HOWARD MC FARLAND
1	DENVER DIVISION MARTIN MARIETTA CORPORATION P. O. BOX 179 DENVER, COLORADO 80201	DR MORGANTHALER A. J. KULLAS
1	ASTROPOWER LABORATORY MC DONNELL-DOUGLAS AIRCRAFT COMPANY 2121 PAULARINO NEWPORT BEACH, CALIFORNIA 92663	DR. GEORGE MOC DIRECTOR, RESEARCH
1	MCDONNEL-DOUGLAS AIRCRAFT CORP. P. O. BOX 516 MUNICIPAL AIRPORT ST. LOUIS, MISSOURI 63166	R. A. HERZMARK
1	MISSILE AND SPACE SYSTEMS DIVISION MC DONNELL-DOUGLAS AIRCRAFT COMPANY 3000 OCEAN PARK BOULEVARD SANTA MONICA, CALIF. 90406	MR. R. W. HALLET CHIEF ENGINEER ADV. SPACE TECH.
1	SPACE+INFORMATION SYSTEMS DIVISION NORTH AMERICAN ROCKWELL 12214 LAKEWOOD BOULEVARD DOWNEY, CALIFORNIA 90241	LIBRARY

1	ROCKETDYNE (LIBRARY 586-306) 6633 CANOGA AVENUE CANOGA PARK, CALIF. 91304	DR. R. J. THOMPSON S. F. IACOBELLIS
1	NORTHROP SPACE LABORATORIES 3401 WEST BROADWAY HAWTHORNE, CALIFORNIA 90250	DR. WILLIAM HOWARD
1	ROCKET RESEARCH CORPORATION 520 SOUTH PORTLAND STREET SEATTLE, WASHINGTON 98108	FOY MCCULLOUGH, JR.
1	SUNSTRAND AVIATION 2421 11TH STREET ROCKFORD, ILLINOIS 61101	R. W. REYNOLDS
1	TRW SYSTEMS GROUP TRW INCORPORATED ONE SPACE PARK REDONDO BEACH, CALIF. 90278	G. W. ELVERUM
1	THIOKOL CHEMICAL CORPORATION HUNTSVILLE DIVISION HUNTSVILLE, ALABAMA 35807	JOHN GOODLOE
1	RESEARCH LABORATORIES UNITED AIRCRAFT CORP. 400 MAIN ST. EAST HARTFORD, CONN. 06108	ERLE MARTIN
1	HAMILTON STANDARD DIVISON UNITED AIRCRAFT CORP. WINDSOR LOCKS, CONN. 06096	MR. R. HATCH
1	UNITED TECHNOLOGY CENTER 587 METHILDA AVENUE P. O. BOX 358 SUNNYVALE, CALIFORNIA 94088	DR. DAVID ALTMAN
1	FLORIDA RESEARCH AND DEVELOPMENT PRATT AND WHITNEY AIRCRAFT UNITED AIRCRAFT CORPORATION P. O. BOX 2691 WEST PALM BEACH, FLORIDA 33402	R.J. COAR
1	DYNAMIC SCIENCE 2400 MICHELSON DR. IRVINE, CALIFORNIA, 92664	DR. J. KLIEGEL